2008

Paleoseismic investigation of the San Andreas Fault, Portola Valley, California

James Aaron Wetenkamp
San Jose State University

PALEOSEISMIC INVESTIGATION OF THE SAN ANDREAS FAULT,

PORTOLA VALLEY, CALIFORNIA

A Thesis

Presented to

The Faculty of the Department of Geology

San José State University

In Partial Fulfillment

of the Requirements for the Degree

Master of Science

by

James Aaron Wetenkamp

May 2008

UMI Number: 1458147

UMI®

UMI Microform 1458147

ProQuest Information and Learning Company
300 North Zeeb Road
P.O. Box 1346
Ann Arbor, MI 48106-1346

APPROVED FOR THE DEPARTMENT OF GEOLOGY

Dr. John W. Williams

Dr. Richard L. Sedlock

Dr. Carol S. Prentice, U. S. Geological Survey, Menlo Park, California

APPROVED FOR THE UNIVERSITY

04/30/08

ABSTRACT

PALEOSEISMIC INVESTIGATION OF THE SAN ANDREAS FAULT, PORTOLA VALLEY, CALIFORNIA

James A. Wetenkamp

Very few data are available regarding the recurrence interval and behavior of the Peninsula segment of the San Andreas Fault. Additional data are required to accurately describe the history and characteristics of slip on the fault. Trenching perpendicular across the fault in Portola Valley, California has provided insight into the timing of surface rupture earthquake events (such as the April 18, 1906 earthquake).

The trench revealed scarp-derived colluvial wedges that overlie and interfinger with Holocene fluvial deposits. The data indicate an average recurrence interval of approximately 292 years and a penultimate event date of 1400 A.D. or later. These data correlate well with data from previous studies that show a penultimate 1906-type earthquake on the northern section of the SAF occurring between 1655 and 1588.

ACKNOWLEDGEMENTS

I would like to thank Carol Prentice of the USGS and John Baldwin of William Lettice and Associates for all their assistance on this project. Without the experience of both Carol and John, I would have been lost in the trenches, and would have never seen the important things that we found. I would also like to thank the property owners for allowing us to do research on their property. Dr. John Williams and Dr. Richard Sedlock were also very instrumental in the completion of this thesis. Their constructive criticism helped to guide me in the right direction.

I am indebted to Nan and Rob Shostak for providing me with a place to live less than a mile away from the project site. It would have been much more difficult for me to commute every day 2 ½ hours to and from the site.

I cannot forget to thank my wife and my daughters, Lindsey, Natalia, and Gwen, for their patience throughout graduate school. It has been a long and difficult road to get to this point, and they have been very supportive of everything I had to do. Finally, I would like to thank the man responsible for the beautiful weather that was provided during the entire time the trenches were open. The only rain came on the day the trenches were closed.

TABLE OF CONTENTS

LIST OF FIGURES

LIST OF TABLES

LIST OF PLATES

INTRODUCTION

Although motion between the Pacific and North American plates is accommodated by a wide zone of faulting and deformation from offshore of the California coastline through the Basin and Range province, the San Andreas Fault (SAF) system (Fig. 1) commonly is recognized as the principal slip structure between the two plates (Kelson et al., 1992). The SAF zone extends 1,100 km from the Mendocino triple junction to the Salton Sea (Bryant and Lundberg, 2003). The purpose of this study is to expand the understanding of the behavior of seismic activity on the San Francisco Peninsula segment of the SAF (SAP) (Fig. 2). To accomplish this goal, a paleoseismic investigation was conducted in the town of Portola Valley, which is located near the center of the SAP (Fig. 3). This thesis presents the results of this study and compares them to the published results of other recent, nearby paleoseismic studies on the SAP.

The SAF system accommodates approximately 80% of present day dextral transform motion between the Pacific and North American plates (Argus and Gordon, 1991). However, the SAP has not experienced a surface-rupturing earthquake since April 18, 1906 (Bryant and Lundberg, 2003).

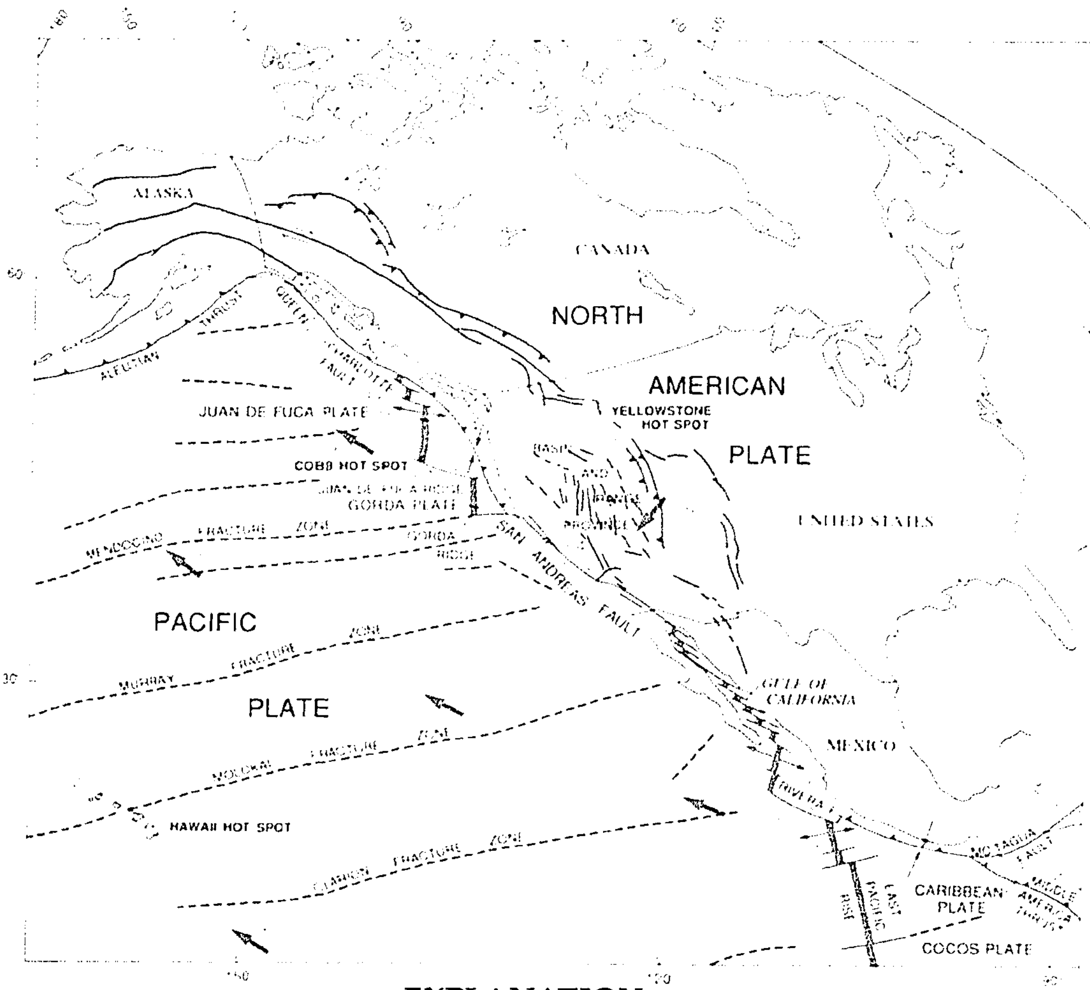

EXPLANATION

Strike-slip fault - Showing slip vectors and rate (cm/yr)

Subduction zone - Showing slip vectors and rate (cm/yr) of convergence; sawteeth on upper plate

Spreading center - Showing vectors and rate (cm/yr) of spreading

Vector and rate (cm/yr) of absolute plate motion

Hot spot and vector of plate motion relative to it

Fracture zone in Pacific plate

Fault in North American plate - Sawteeth on upper plate of thrust fault

Figure 1. The San Andreas Fault system (Wallace, 1990)

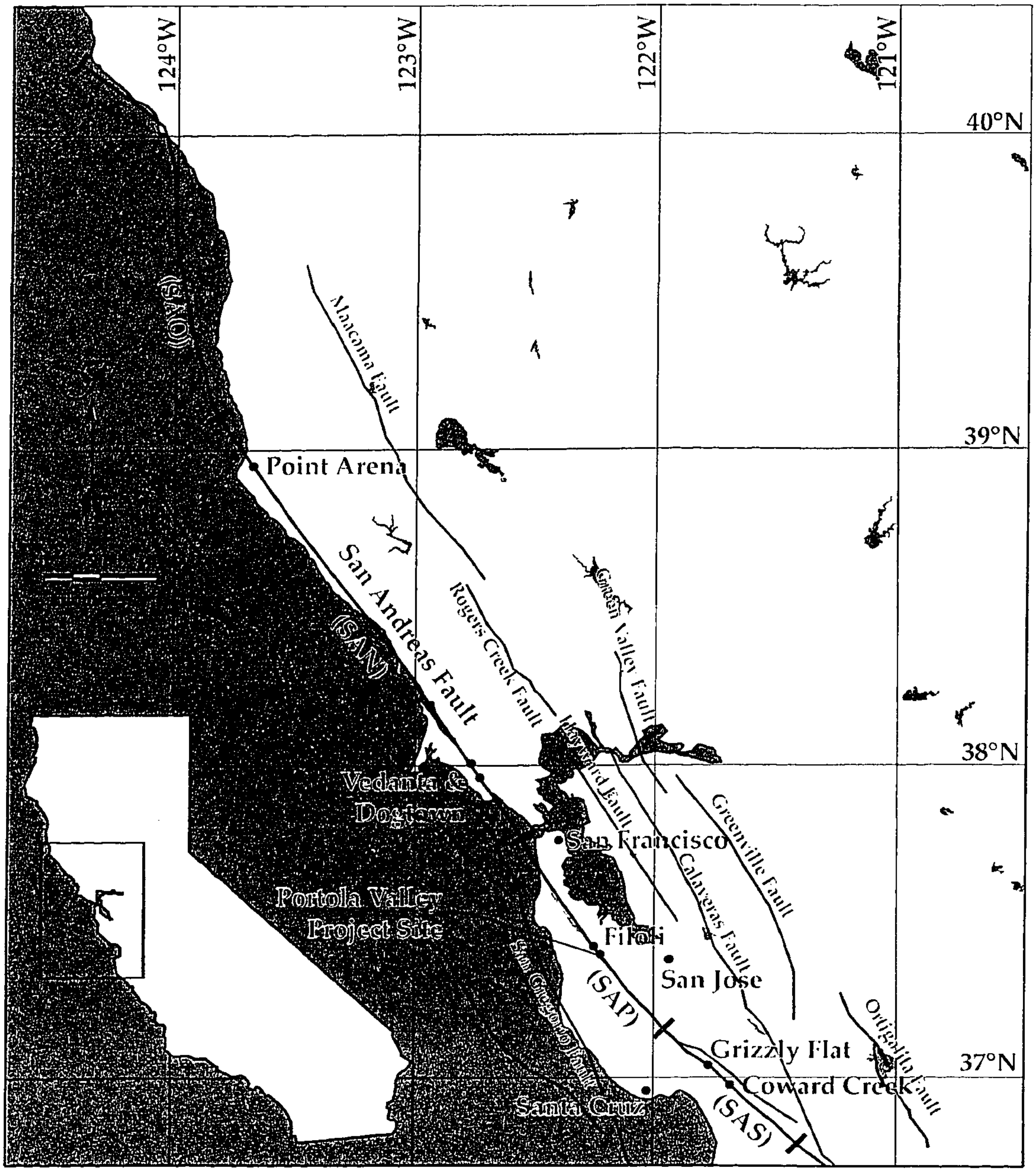

Figure 2. The San Andreas fault segments. San Andreas Offshore (SAO), San Andreas Northern (SAN), San Andreas Peninsula (SAP), and San Andreas Santa Cruz Mountains (SAS). Modified from Working Group on California Earthquake Probabilities (2003).

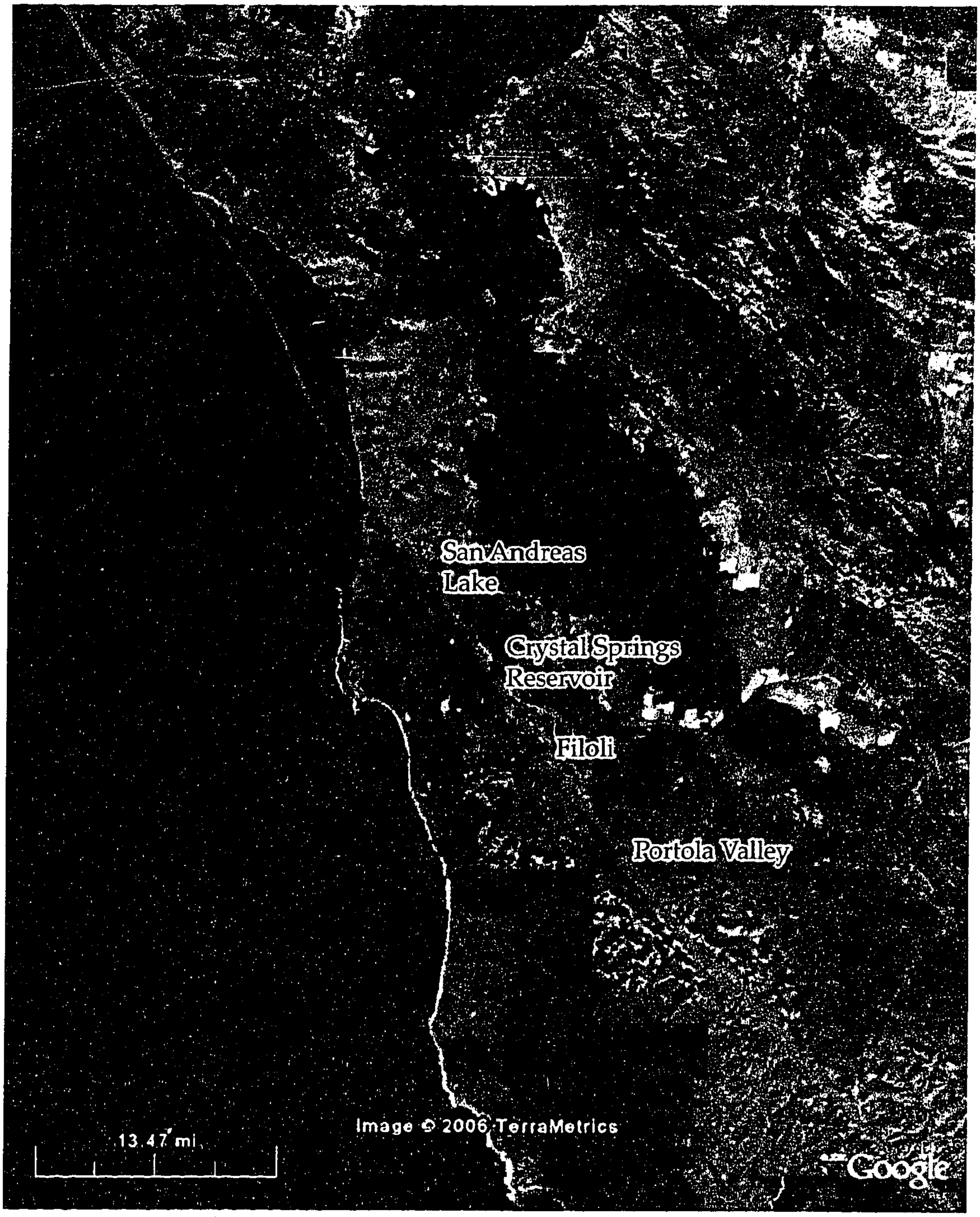

Figure 3. The Peninsula Segment of the San Andreas Fault. Here, the fault passes through San Andreas Lake, Crystal Springs Reservoir, Filoli and Portola Valley. Modified Google Earth image, 2006 (used with permission). Fault lines obtained from the United States Geological Survey (ftp://hazards.cr.usgs.gov/maps/qfault/, dated March 2006).

After more than 100 years without slip on the SAP, many geologists and bay area residents are wondering if the peninsula is due for a large surface-rupturing event (WGCEP, 2003). An important aspect of fault behavior is the recurrence interval between large destructive earthquakes. A goal of this study is to update or confirm the currently accepted recurrence interval for large, surface rupturing earthquakes on the SAP. WGCEP (2003) reports an estimated recurrence interval of 225 years for the SAP, and a recurrence interval of 180-370 years for 1906-type events that rupture multiple segments of the SAF.

THE SAN ANDREAS FAULT SYSTEM

With its numerous faults and active plate boundary, California has become a major focus for the study of faults. Following the devastating earthquake of April 18, 1906, Andrew C. Lawson orchestrated the first comprehensive study of the SAF. This study was published in 1908 as *The California Earthquake of April 18, 1906, Report of the State Earthquake Investigation Commission* (Lawson, 1908). Since then, many researchers have published studies that have greatly enhanced our understanding of the development and history of the SAF (Hill and Dibblee, 1953; Sarna-Wojcicki, 1992; Atwater and Stock, 1998; Wakabayashi, 1999; Argus and Gordon, 2001).

Evolution of the San Andreas Fault

The San Andreas Fault system owes its beginnings to the interactions between the Pacific and North American plates. About 30 million years ago, the subduction zone west of North America began to be replaced by a transform boundary between the North American and Pacific plates (Fig. 4). Most geologists agree that displacement on the SAF began approximately 18 Ma (Atwater and Stock, 1998; Wakabayashi, 1999) with most of the offset taking

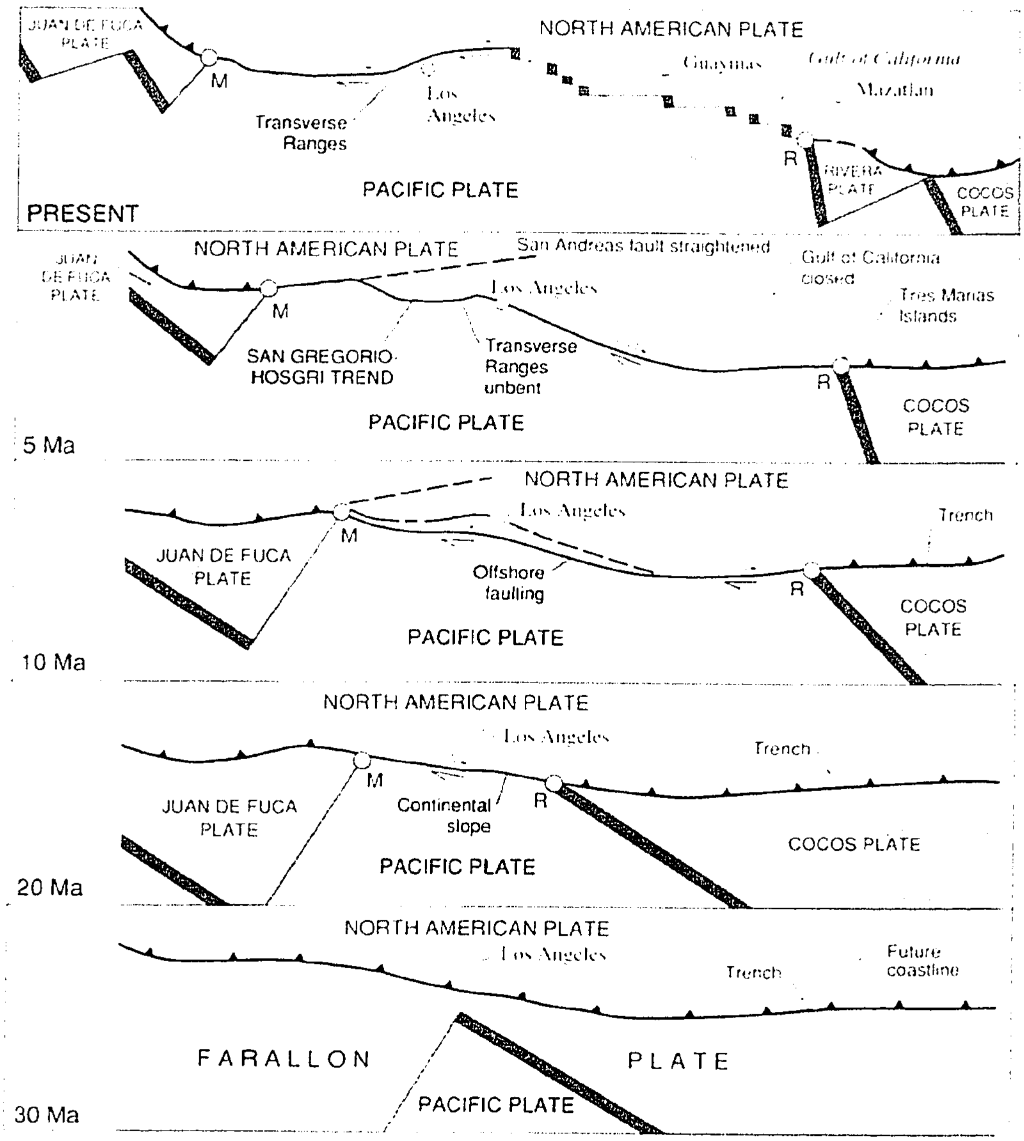

Explanation

Spreading center

Subduction zone - Dashed where approximately located. Sawteeth on upper plate.

Fault - Dashed where approximately located. Arrows indicate direction of relative movement.

O M **Mendocino triple junction**

O R **Rivera triple junction**

Figure 4. Progression of the formation of the San Andreas Fault. Modified from Wallace, 1990.

place within the last 5 million years (Bohannon and Parsons, 1995; Irwin, 1990).

It has been shown that offset of greater than 300 km has occurred along the SAF since its inception (Wakabayashi, 1999, Sarna-Wojcicki, 1992, Irwin, 1990). Collectively, the SAF System (Fig. 2), from faults offshore of California to the Ortigalita and related faults, record offset of as much as 590 km (Wakabayashi, 1999).

General Fault Characteristics

Geomorphology

On a shaded relief map of California (Fig. 5), the San Andreas fault zone can be seen as a linear feature that runs almost the entire length of the state. It is expressed as a series of linear ridges and valleys within the Coast Ranges of northern and central California and the Transverse Ranges in southern California. The linear valleys, such as Portola Valley, are the result of a variety of processes such as differential weathering of the soft, sheared material within the fault zone. Linear ridges can be formed due to transpression along a bend in the fault, such as the Transverse Ranges. Differential erosion of juxtaposed rocks can also create a linear ridge.

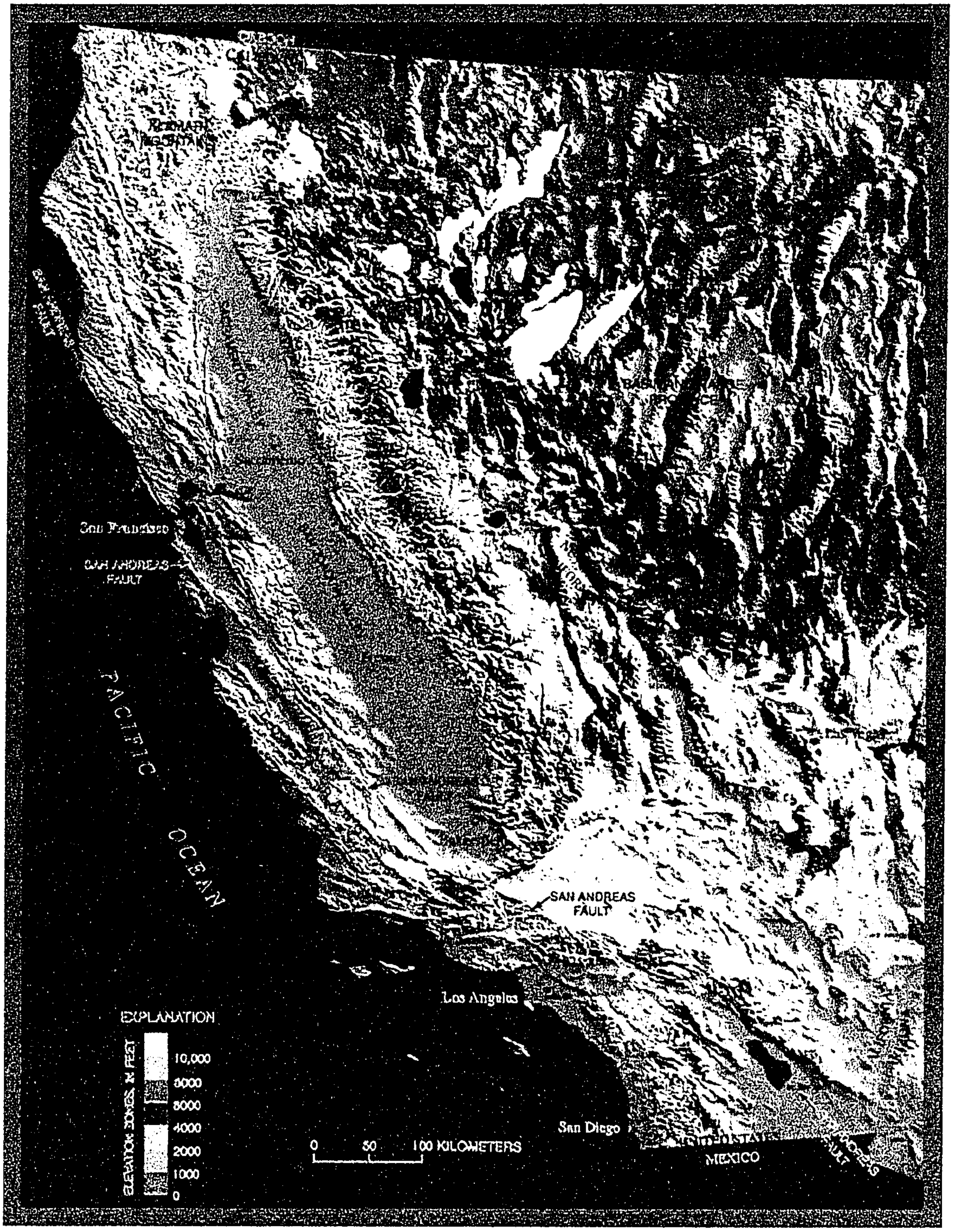

Figure 5. Shaded relief map of California. Modified from Wallace, 1990.

On a larger scale many other geomorphic features can be seen, including offset streams, beheaded streams, sag ponds, shutter ridges, and scarps (Fig. 6, Wallace, 1990). A more complete discussion of these features as they are observed on the SAP can be found below.

Offset Geologic Features

Several of the more compelling pieces of evidence for large scale displacement on the SAF are the Neenach Volcanic Formation and the Pinnacles Volcanic Formation, the Butano Sandstone and the Point of Rocks Sandstone Member of the Kreyenhagen Formation, and the Roblar Tuff (Fig. 7). Based on these geologic features, the main trace of the SAF system in northern California has been estimated to have a dextral offset of 228 ± 13 to 315 km (Sarna-Wokcicki, 1992; Irwin, 1990).

Segmentation of the San Andreas Fault

The Working Group on California Earthquake Probabilities (WGCEP) defines a fault segment as "the shortest section considered capable of repeatedly rupturing to produce a large earthquake" (WGCEP, 2003).

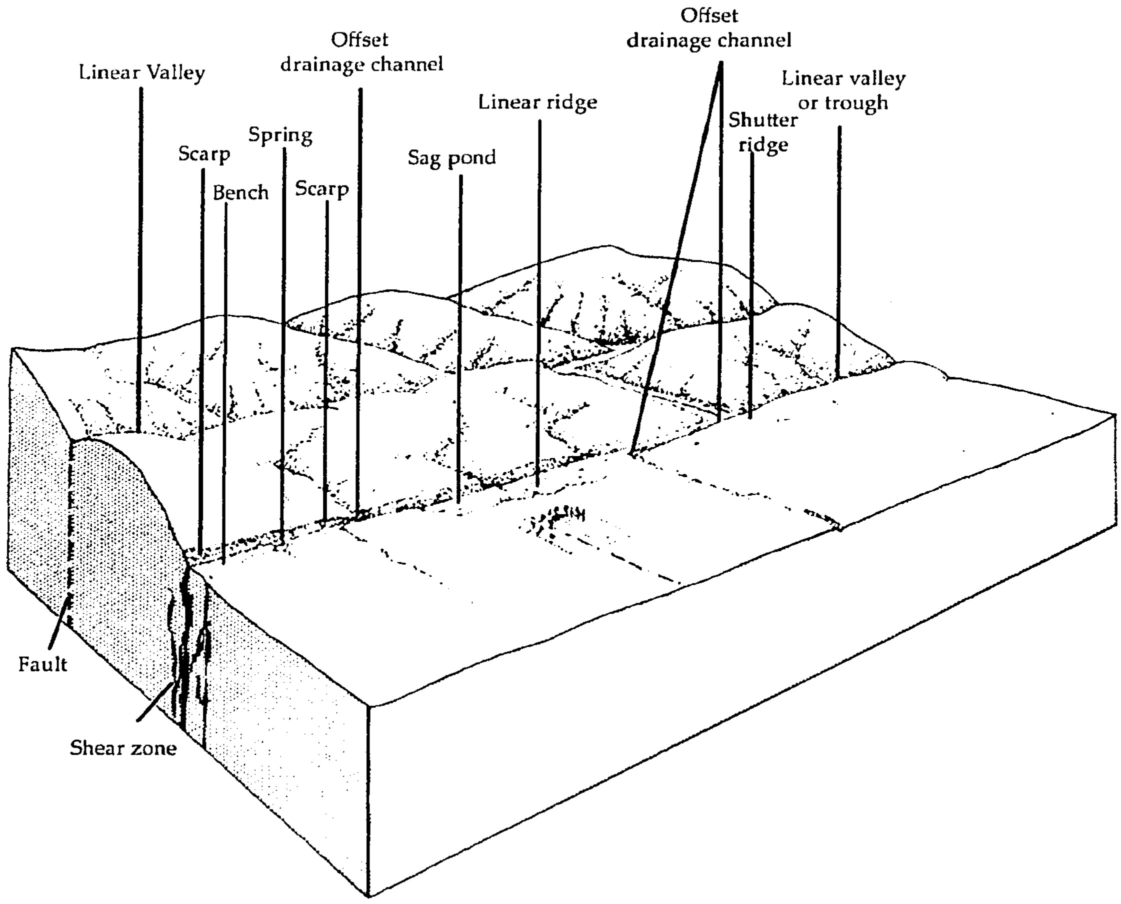

Figure 6. Common geomorphic features of strike slip faults. Modified from Wallace, 1990.

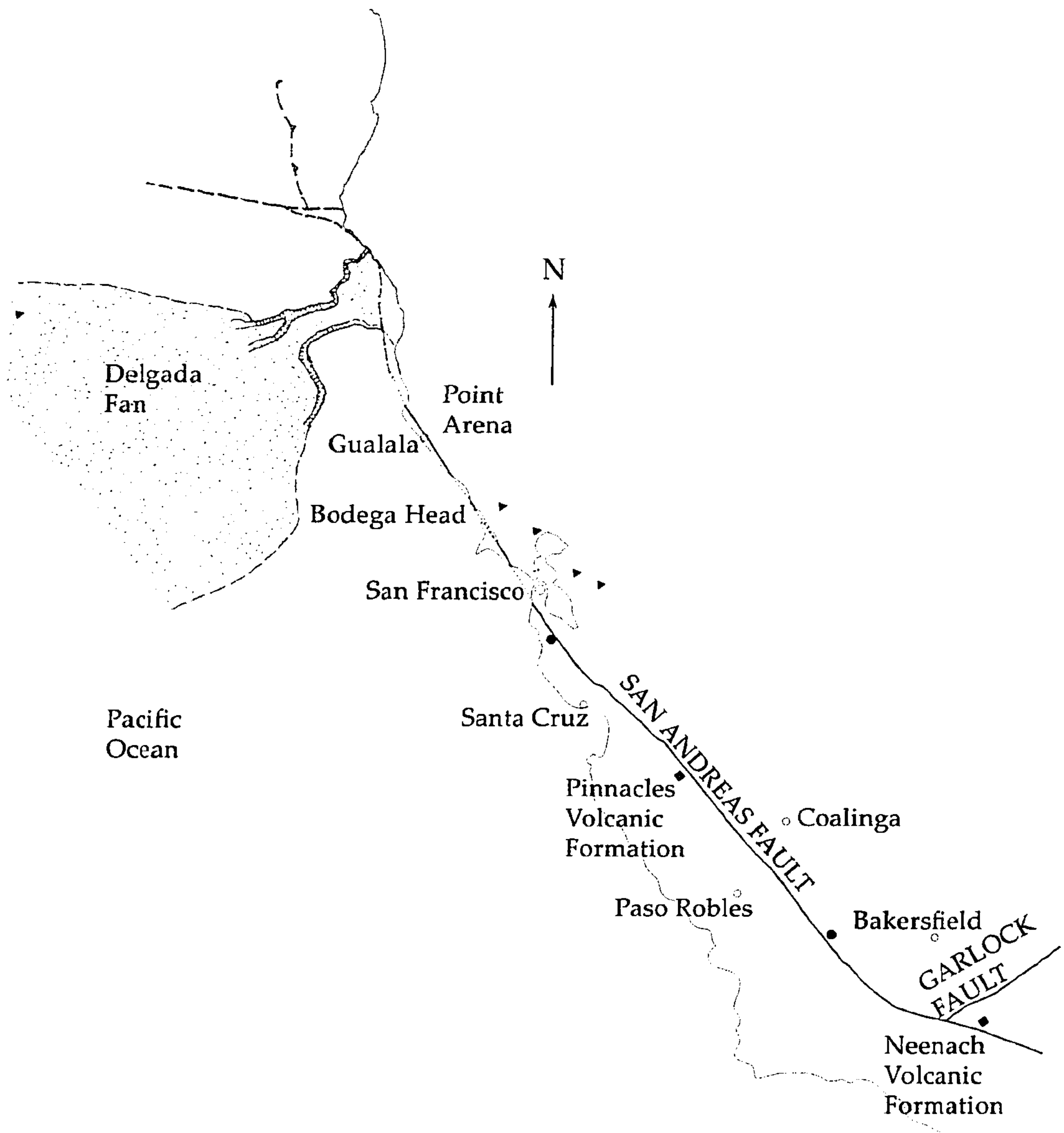

Figure 7. Offset features on the San Andreas Fault. These features have been mapped by various authors. The squares show the locations of the Pinnacles and Neenach Volcanic Formations. The dots show the locations of the Butano Sandstone and Point of Rocks Sandstone Member (of Kreyenhagen Formation), representing offset parts of an Eocene deep-sea fan. The triangles show the locations where the Roblar tuff has been found. Modified from Wallace, 1990 and Sarna-Wojcicki, 1992.

Fault segment boundaries are identified based on two criteria: the physical properties of the fault and the behavior of the fault. Some of the physical properties of faults that determine segmentation are the locations of bends, steps, branches, intersections, and changes in fault complexity and lithology. Behaviors of faults that determine segmentation include slip rates, slip type (i.e., seismic or creep), ground rupture, and paleoseismic/historic activity (WGCEP, 2003).

Using these criteria, the WGCEP has divided the northern SAF into four segments (Fig. 2). Portola Valley is on the Peninsula segment of the SAF (Fig. 2). The northern boundary of the SAP lies near the Golden Gate Bridge where the San Gregorio fault intersects the SAF (WGCEP, 2003). This boundary is marked by a decrease in offset observed from the 1906 earthquake, and a possible decrease in the late Holocene slip rate by about 7 mm yr^{-1} (WGCEP, 2003). The southern boundary of the SAP is 85 km southeast of its northern boundary, near Los Gatos (Fig. 2). A restraining bend in the fault marks the southern boundary of the SAP and the northern end of the Loma Prieta aftershock zone (WGCEP, 2003).

The late Holocene slip rate on the SAP is slightly lower than on the segments of the SAF to the south. Hall et al. (1999) calculated a slip rate range for the SAP of 17 ± 4 mm yr^{-1} from dates and distances of offset stream channels at the Filoli Center, north of Woodside, CA (Fig. 3). This slip rate is slower than that of some estimates of the Santa Cruz Mountains (SAS) segments of the SAF. On the SAS an average slip rate has been calculated to be approximately 22 mm yr^{-1}. This slip rate deficit on the SAP is either being accommodated by deformation or slip on other San Francisco Bay region faults. The slip rate on the SAN, as determined by Noller et al. (1996) and Prentice (1989), ranges from 16 to 27.5 mm yr^{-1}, respectively. More recent work however, suggests no significant difference in slip rate between the SAP and the SAN (Prentice et al., 2001).

Characteristics of the SAP

On the ground the SAF is not a continuous heavy black line across California as seen on maps. At a larger scale, smaller geomorphic features can be identified and a more realistic understanding of the fault's geometry and its behavior can be attained.

Geomorphology

The San Francisco peninsula has an abundance of geomorphic features that mark the location of the SAF. Many of the features that were observed by Lawson and his associates have been covered by homes, shopping centers, and a school or two (Pampeyan, 1995). Pampeyan's (1995) map of the SAP with its various geomorphic and historic features was prepared using pre-development aerial photographs and published and unpublished comments by Lawson and his associates followed by ground reconnaissance. Although many surface expressions of the fault have been erased, some have been spared and can still be seen today. Much of the southern reach of the SAP is located in undeveloped or preserved areas, such as Portola Valley.

Sag ponds are abundant in the less populated areas along the trace of the fault, and can be seen in aerial photos and identified in the field as low-lying marshy areas or locations with standing water. Offset streams and shutter ridges are also present on the peninsula (Pampeyan, 1995). Several small but prominent scarps are located southeast of Upper Crystal Springs Reservoir (Pampeyan, 1995).

En Echelon Fractures

As observed by Lawson (1908) and others, the SAF is not always expressed as a single through-going fracture at the surface of the Earth. In many places en echelon fractures are observed instead (Fig. 8). Lawson described a set of en echelon fractures in Portola Road, just north of the study site of this thesis:

> The main fault fracture passes through the Portola Valley and crosses the public road in front of a small 1-story house southeast of the village store. Where the fault crosses the road, the fences on both sides were torn in two, and in the prune orchard south of the road the rows of trees were displaced in some instances about 2 feet. The cracks in the road were about 6 inches wide, approximately parallel, and running nearly north-south, while the direction of the fault line itself was about northwest-southeast. (Lawson, 1908)

Other locations of en echelon faulting on the SAP have been mapped by Pampeyan (1995).

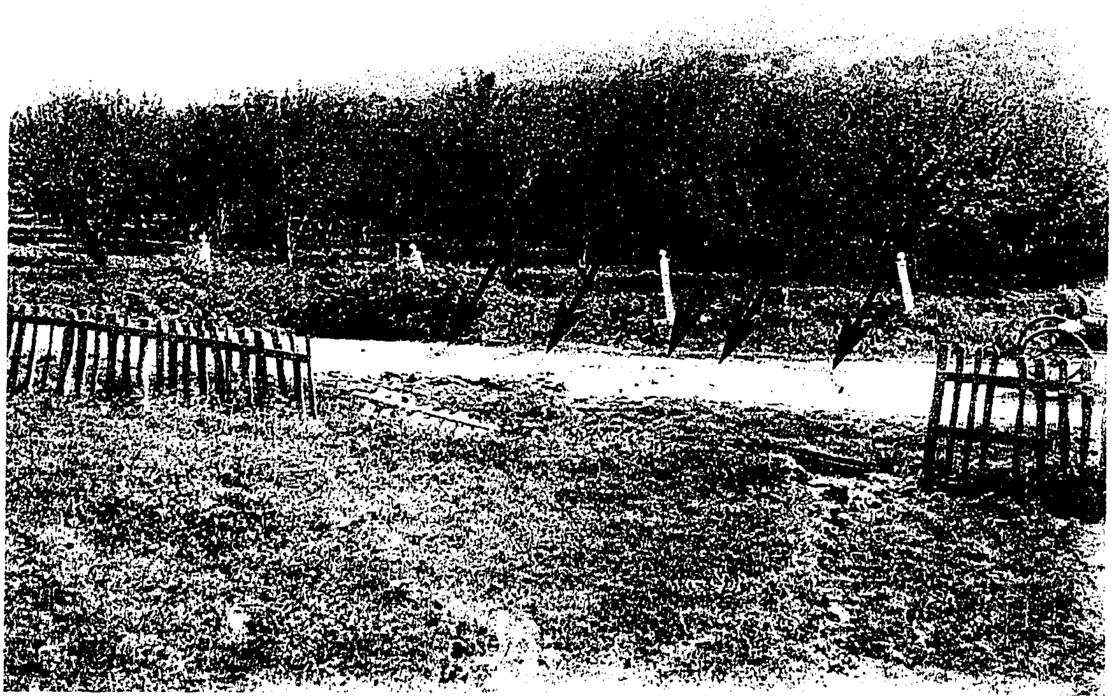

Figure 8. Photograph of the 1906 Fault Rupture in Portola Valley. The arrows point to the surface ruptures in Portola Road. Courtesy of the U.S. Geological Survey.

Multiple Fault Traces

In places, slip along one fault trace dies out and is transferred to a subparallel trace several hundred meters or more away (Fig. 9). This can occur as a step-over during a single surface rupturing event or over large periods of time as slip stops on one trace and is transferred onto another trace.

In Portola Valley, multiple traces of the SAF have been mapped (Figs. 9, 10 and 11). The Woodside trace is the trace that ruptured during the 1906 earthquake. Fisher et al. (2002) found evidence for recent activity on the Trancos trace southeast of the Portola Valley Town Center. Preliminary results of their study of the Trancos trace found Holocene faulting and soil development indicating activity as young as 1,400 years B.P. (Fisher et al., 2002).

A third unnamed fault trace in Portola Valley is mapped on the California Geological Survey Special Study Zones map for the San Andreas Fault, Palo Alto 7.5-minute quadrangle (CGS, 1974) near the western boundary of the A-P fault zone. It had been mapped from aerial photos that showed a subtle lineament. This lineament was explored through trenching by William Lettis and Associates (2004) to a depth of 3.5 meters. No evidence for surface faulting in the Holocene was found, and it was concluded that the fault was inactive or non-existent.

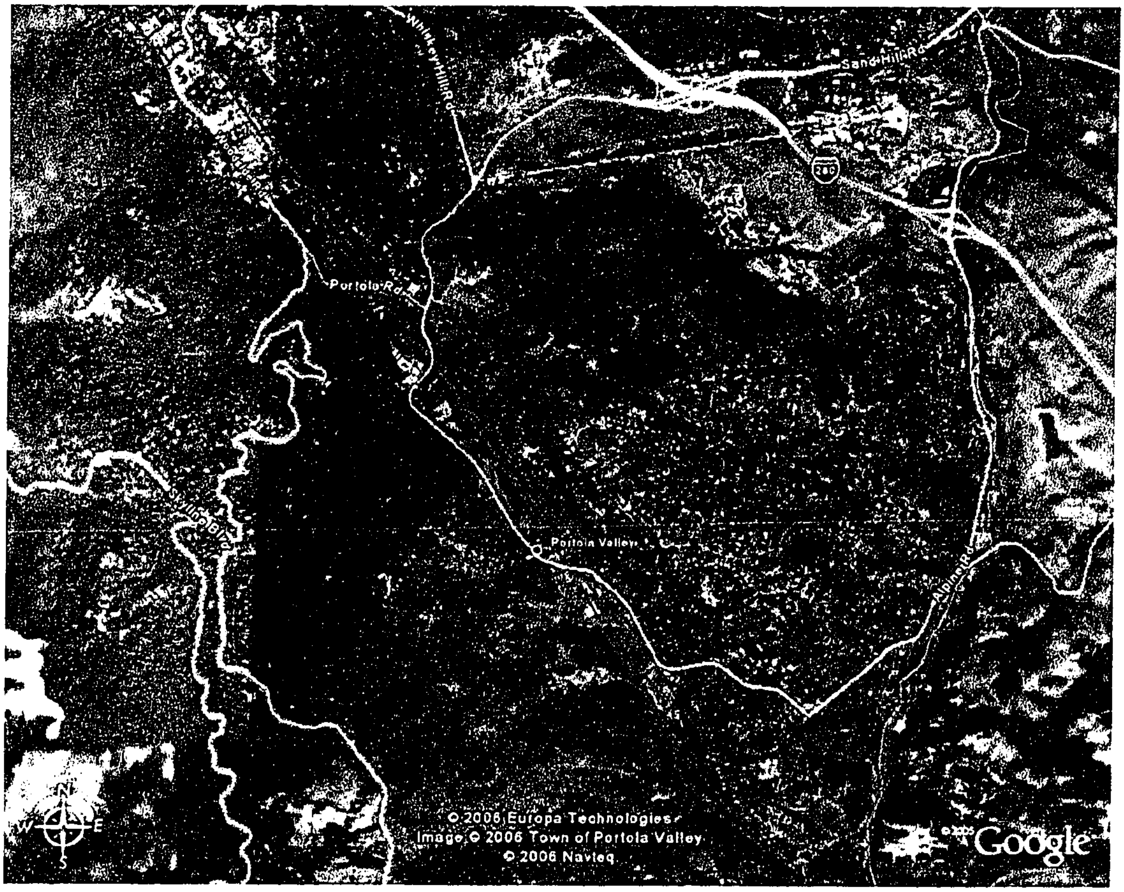

Figure 9. Multiple Traces of the San Andreas Fault. This Google Earth aerial photograph includes an overlay of multiple traces of the San Andreas Fault that was produced by the US Geological Survey (ftp://hazards.cr.usgs.gov/maps/qfault/, dated March2006). Google Earth image, 2006 (used with permission).

SEISMIC ACTIVITY ON THE PENINSULA SEGMENT OF THE SAN ANDREAS FAULT

Hundreds of kilometers of offset have occurred along the SAF. There is no doubt that many substantial earthquakes have accompanied this offset in pre-historic time. One of the goals of this study is to understand the history of seismic activity on the SAP so that we can better prepare for future earthquakes.

Pre-Historic Earthquakes

Pre-historic earthquakes are those that occurred prior to recorded (written) history. In California, widespread written records are available from around the mid-1800s when gold was discovered and many people migrated west to seek their fortunes. Prior to this, limited records were kept at the various missions in California; one of the earliest missions, San Francisco Dolores, was built in 1776 (Toppozada, 2002). Mission reports along with the journal entries of several travelers provide shaking and structural damage observations from earthquakes in the San Francisco Bay Area as early as 1781 (Toppozada, 2002).

Specific earthquake/surface rupture events prior to 1838 have been inferred from offset stratigraphic units or other markers that are observed and dated in trenches excavated for paleoseismic investigations. Several other techniques that have been used for identifying and dating paleoseismic events are described below.

Hall (1984) estimated that an offset stream between Crystal Springs Reservoir and San Andreas Lake (Fig. 3) experienced 19 to 32 rupture events similar in size to the 1906 event. This was calculated by dividing the deflection distance (170-285 ft) by the 9-foot displacement that was caused at the site by the 1906 earthquake.

Schwartz and others (1998) combined the data from a trench in the Grizzly Flat area (Fig. 2) of the Santa Cruz Mountains with data from an old redwood tree stump near the site to corroborate dates of a major earthquake. This was done by noting that the years of slow growth in the tree rings coincided with the date of a surface rupturing event identified in the trench. Schwartz then compared his results with the results of other studies on the SAF (Table 4 and Fig. 15) and found an overlap of time in the mid-1600s for which a single 1906-type event could have occurred along the SAF from Point Arena to the Santa Cruz Mountains. An event in the mid-1600s to mid-1700s is commonly accepted as the penultimate 1906 type rupture event (Hall et al., 1999).

Historic Earthquakes

The first earthquake in the San Francisco Bay area for which a written record exists occurred in 1781 (Toppazada, 2000). The first recorded major (M 7 or larger) earthquake in the San Francisco Bay area occurred in 1838. Toppazada (2000) reported from various sources that this earthquake produced a Modified Mercalli Intensity (MMI) of VIII from San Francisco to Gilroy. Based on this evidence, Toppazada (2000) estimates a moment magnitude of 7.4 for this earthquake and suggests that it occurred on the SAF.

The first comprehensive post-earthquake investigation in California was carried out following the San Francisco earthquake of 1906 (Prentice, 1999). This earthquake was associated with fault surface rupture of at least 435 km on four segments of the SAF, the Offshore (SAO), North Coast (SAN), San Francisco Peninsula (SAP), and Santa Cruz Mountains (SAS) segments (Prentice et al., 1999 and Prentice, 1999) (Fig. 2). The moment magnitude for this earthquake has been calculated to be 7.8 (Bakun, 1999).

Since 1906 the SAP has not experienced a surface-rupturing earthquake (Toppazada, 2002). With such limited historical data dating back less than 170 years, it is very difficult to accurately characterize the SAP. Paleoseismic investigations can provide additional data on the character and history of activity on the SAF

Slip Rate Estimates

A slip rate for a fault can be determined in several ways. If the fault is creeping (aseismic slip), offset can be measured by establishing a monitoring system on either side of the zone of active faulting. Measurements are made to determine how much slip has occurred over a period of time, thus providing a rate of slip. This can also be done using the Global Positioning Satellite (GPS) system.

For faults that do not creep, it is necessary to locate a piercing point that can be dated and measured. Hall et al. (1999) used a sequence of channel deposits at the Filoli Center that have been offset by the SAF. Their study recorded an average horizontal slip rate of 17 ± 4 mm yr^{-1} and an average vertical slip rate of approximately 1 ± 0.2 mm yr^{-1}.

Recurrence Interval Estimates

Probability calculations for major earthquakes are based primarily on mean rupture rates and magnitudes (WGCEP, 2003). Thus, it is particularly important to continue to refine the recurrence interval for active faults that are located near densely populated areas. Because the various segments of the SAF behave differently, they have different recurrence intervals. Hall et al. (1999) conducted an extensive paleoseismic study on the SAP near Woodside, California. Based on the evidence found there, Hall suggested a recurrence interval of 250 to 320 years for surface rupturing earthquakes similar to the 1906 event.

WGCEP (2003) found that the recurrence interval for large surface rupturing earthquakes on the Northern SAF (SAO+SAN+SAP+SAS) ranges from 180 to 370 years. However, all of the evidence provided comes from paleoseismic investigations on the SAN and SAS, not the SAP. Obviously more data are needed to calculate a more accurate recurrence interval.

GEOLOGY OF THE SAN FRANCISCO PENINSULA

The geology of the San Francisco Peninsula is complex. Numerous faults have juxtaposed many different rock types that were formed in distant locations by very different processes. The major geologic units that form the basement of the San Francisco Peninsula are the Cretaceous and Jurassic Franciscan Complex and the Cretaceous Salinian Block. These basement rocks have been sheared, faulted, and folded and form the core of the modern Coast Ranges (Page et al., 1998). Some of the more important younger deposits include the Santa Clara Formation, Butano Sandstone, Lambert Shale, Purisima Formation and the Whiskey Hill Formation (Brabb et al., 2000). These younger sedimentary sequences are critical for dating pre-historic surface-rupturing earthquakes on the SAP.

The Franciscan Complex

The Franciscan Complex consists of rocks that collected in the subduction zone at the western edge of the North American plate. Subunits include coherent slabs of metasedimentary and metabasaltic rocks, plus a mélange that contains a variety of blocks, including exotic ophiolite, blueschist and eclogite

(Page et al., 1998). The Franciscan Complex was subsequently thrust onto the North American plate and can now be found throughout the Coast Ranges. The Franciscan Complex is generally east of the SAF, however on the San Francisco Peninsula the Franciscan Complex can be found on both sides of the SAF with its western boundary being the Pillarcitos fault. Based on this information, the Pillarcitos fault is probably an ancient trace of the SAF. The Franciscan Complex has been dated as Late Jurassic to Cretaceous in age (Page et al., 1998).

The Salinian Block

The Salinian Block consists of metamorphic rocks and granitic plutons, and is commonly believed to be a remnant of a magmatic arc. The plutonic rocks vary in composition and age, but are very similar to the plutons in the Sierra Nevada and Peninsular ranges (Page et al., 1998). The metamorphic rocks in the Santa Lucia Range are known as the Sur Series and consist of gneiss, schist, quartzite, and marble. The Salinian Block is typically west of the SAF, and is believed to be in fault contact with the Franciscan Complex. Some of the evidence for a fault contact, rather than a depositional contact, is that the Salinian granitics are younger, and no contact metamorphism is seen in the Franciscan Complex where it abuts the Salinian Block.

Tertiary Sedimentary Deposits

A few of the important Tertiary units on the San Francisco Peninsula include the Pliocene and Upper Miocene Purisima Formation, the Miocene Monterey Formation, the Eocene Butano Sandstone, and the Middle and Lower Eocene Whiskey Hill Formation. These marine sedimentary rocks represent shallow-water, clastic, shelf deposits and deep-water, shelf or slope basin sediments (Page et al., 1998). Clarke and Nilsen (1973) suggested that the Twobar Shale Member of the San Lorenzo Formation and the Butano Sandstone, which are found on the west side of the SAF near Portola Valley, correlate to the shale member and the Point of Rocks Sandstone Member of the Kreyenhagen Formation, respectively, which are found on the east side of the SAF near Bakersfield (Fig. 7). This indicates about 305 km of offset along the SAF (Irwin, 1990).

Quaternary Sedimentary Deposits

The Quaternary sedimentary deposits consist generally of gravels, sands, silts, and clays of fluvial origin and include deposits such as the Santa Clara Formation. Because their lower members commonly contain marine deposits, they are interpreted as representing uplift of the continent and the retreat of the ocean (Page et al., 1998). The retreat of the sea lowered the base levels of rivers and streams, which caused erosion that produced the abundant fluvial deposits of the Pliocene and Pleistocene.

LOCAL GEOLOGY OF PORTOLA VALLEY

The geologic features of Portola Valley are controlled primarily by the SAF, which lies near the axis of the valley. Portola Valley is a linear valley situated between the Santa Cruz Mountains on the west and tectonically controlled linear ridges on the east.

Depositional Environment

The Santa Cruz Mountains near the town of Portola Valley receive an average of 30 inches of rain per year. This moderate rate of precipitation generates significant erosion in the mountains, and thus abundant quantities of fluvial material in the valley. Sediment laden streams have built alluvial fans where their gradients decrease near the valley floor.

Portola Valley is underlain by many relatively thin strata that were deposited in several environments. Sausal Creek meanders between the margins of the valley, leaving evidence of its past locations in the form of abandoned stream channel deposits and overbank deposits from floods. During prolonged periods of soil saturation, the valley was in a state of marsh-like conditions that resulted in the deposition of high concentrations of organic matter.

Lithology

The geology of Portola Valley has been mapped by several authors. A 1970 geologic map prepared for the Town of Portola Valley (Dickinson, 1970) (Fig. 10) shows that the valley is filled with Quaternary alluvium and active and inactive landslide deposits. Near the subsurface explorations for this study, the Town Geologic Map shows the Eocene Butano Sandstone. In contrast, recent maps by Pampeyan (1993) and Brabb et al. (2000) show the Whiskey Hill Formations (Fig. 11). The two units are very similar in composition. Both units are described by Brabb et al. (2000) as a light-gray to buff arkosic sandstones. The differences between the two units are the interbedded layers of differing material. The Butano Sandstone is interbedded with mudstone, shale, and conglomerate, whereas the Whiskey Hill Formation is interbedded with silty claystone, glauconitic sandstone, and tuffaceous siltstone. Other units mapped within Portola Valley include the Monterey Formation, the Purisima Formation, the Santa Clara Formation, and unnamed old alluvial fan deposits.

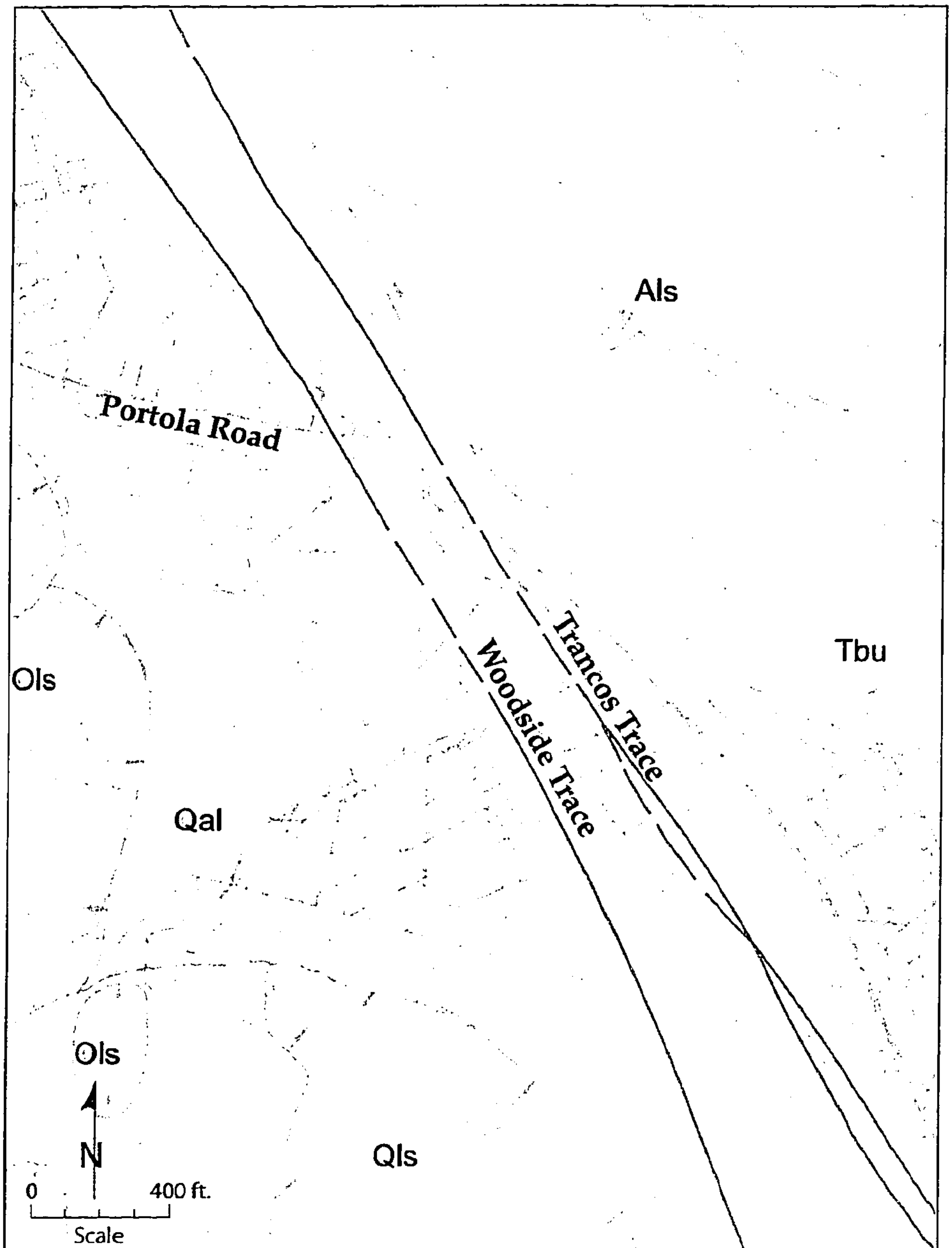

Legend

Als - Active Landslide
Ols - Old Landslide
Qls - Quaternary Landslide
Tbu - Eocene Butano Sandstone

Fault

Dashed where approximately located

Figure 10. Town of Portola Valley Geologic Map. This map by shows the Woodside and Trancos traces of the San Andreas Fault. Modified from Dickenson, 1970.

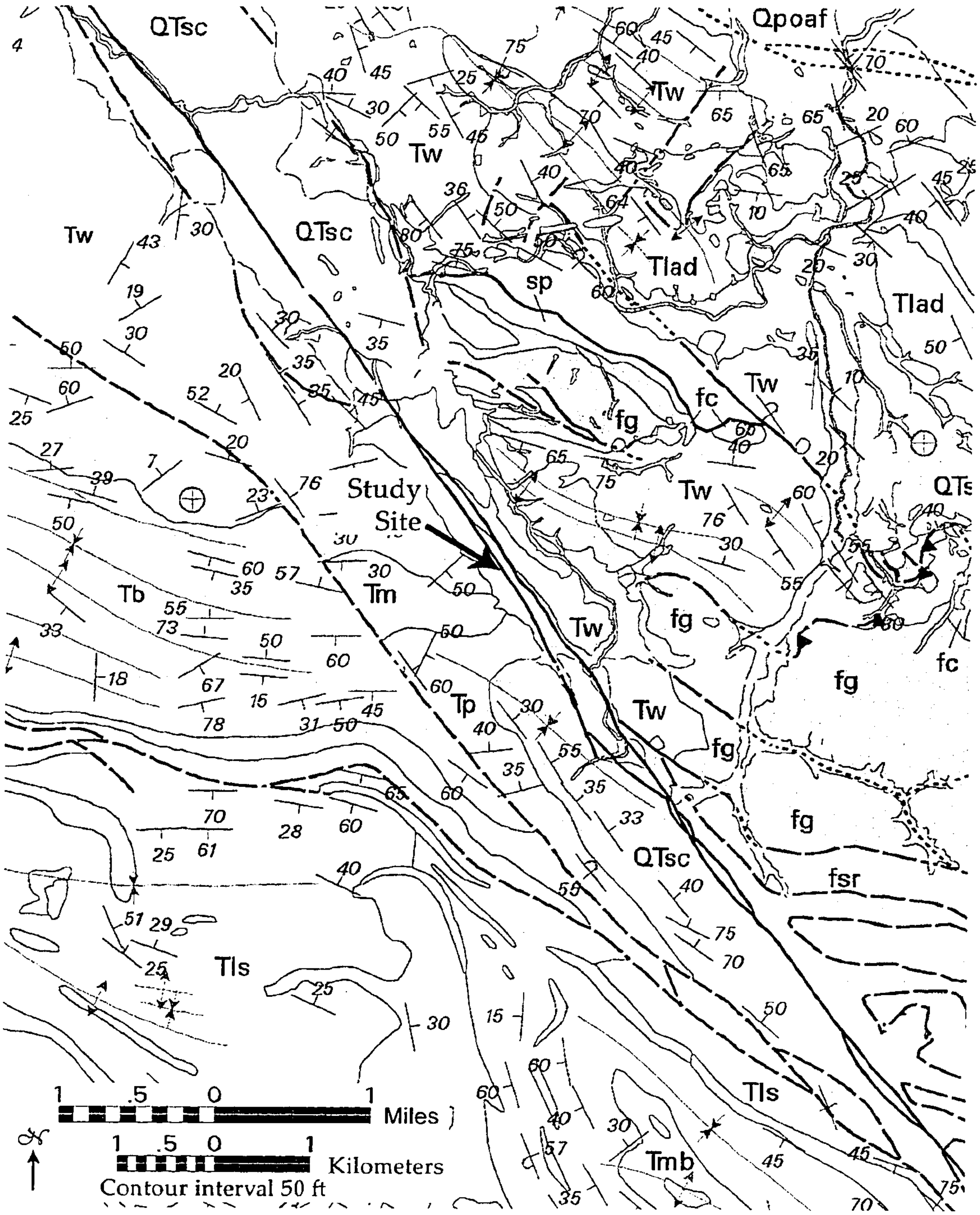

Figure 11. A Portion of the Geologic Map of the Palo Alto Quadrangle. This map by Brabb et al. (2000) shows that the study site is underlain by Quaternary alluvium at the surface and by the Whiskey Hill Formation at depth.

Structure

Portola Valley is an example of a linear valley associated with strike-slip faulting (Fig. 12). The Santa Cruz Mountains west of the valley are about 500 meters higher than the valley floor, whereas the small ridge east of Portola Road is about 30 meters above the valley floor. Similar linear ridges can be found in many places along the SAF and other strike-slip faults, and are diagnostic of the fault's location.

A slight bend to the right in the SAF in Portola Valley creates a pull-apart basin near the study site (Wright et al., 2001) (Fig. 11). The pull-apart basin could be partly responsible for the thick sequence of sediment that overlies the basement rock within Portola Valley. Soil borings drilled southeast of the Portola Valley town center extended to a maximum depth of approximately 27 meters and did not encounter bedrock (William Lettis and Associates, 2004).

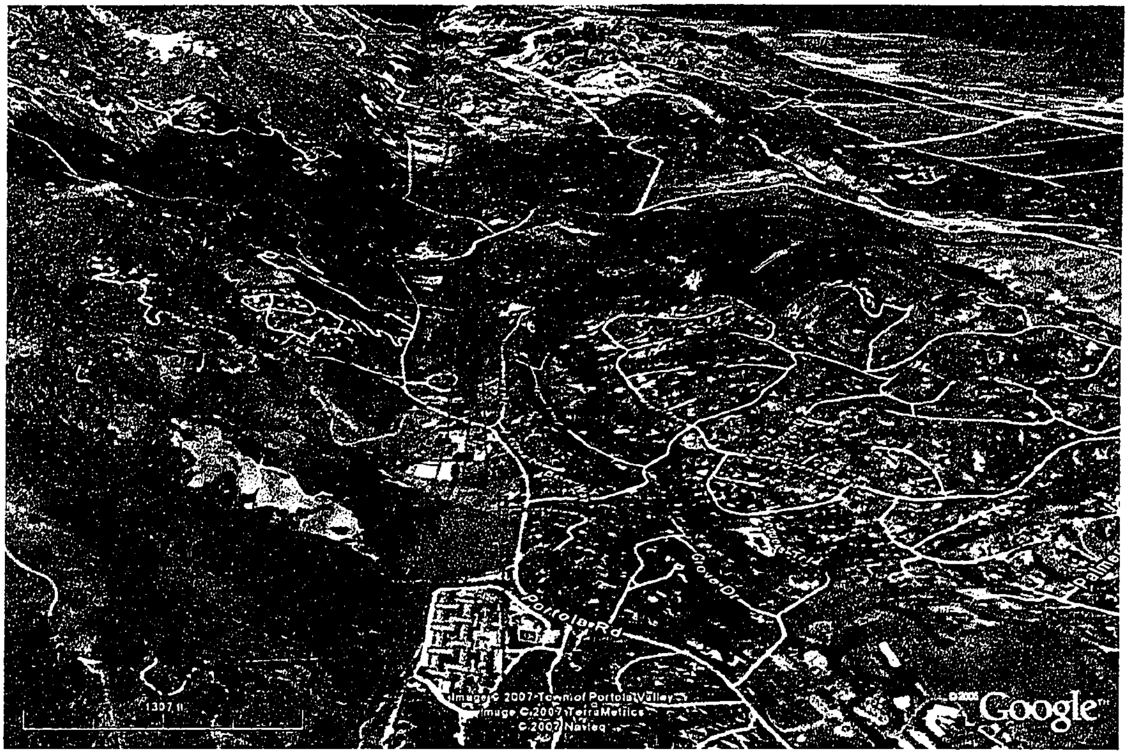

Figure 12. Oblique Aerial View of the Linear Portola Valley. This aerial photograph shows the Santa Cruz Mountains to the west of the fault and a small linear ridge to the east of the fault (fault lines obtained from USGS, ftp://hazards.cr.usgs.gov/maps/qfault/, dated March 2006). 2006 Google Earth image (used with permission).

PRIOR INVESTIGATIONS

Numerous geologic investigations have been conducted on the SAP, including several in and near Portola Valley. Representative of these are Lawson (1908), Taylor and others (1980), Hall (1984), Hall et al. (1999), and William Lettis and Associates, Inc. (2004). These and other investigations on the SAP have greatly enhanced our understanding of earthquakes and faulting in the San Francisco Bay Area.

The First Comprehensive San Andreas Fault Study

After the great San Francisco earthquake of April 18, 1906, Andrew C. Lawson organized a team of geology students and professors to complete a field investigation of the surface rupture. They were charged with documenting all surface expressions of the rupture, which were later compiled into a book (Lawson, 1908). At the time of the investigation very little was understood about earthquakes and their relationship to faults. Strike-slip faulting was even less understood, and was not a widely accepted concept (Prentice, 1999). However, after the event of 1906, there was undeniable proof of strike slip movement on a fault and earthquakes were irrefutably linked to fault activity.

Lawson and his team of investigators made observations of surface rupture from Point Delgada to San Juan Bautista, a distance of about 435 kilometers. The observations, insights, and analyses made during their investigation have proven to be of great value to current seismic hazards analysis. Significant advances in seismology, earthquake geology, and tectonic geodesy have been made as a result of the report (Prentice, 1999).

Portola Valley Study

Several trenches were excavated in Portola Valley across the Woodside and Trancos Traces of the SAF for this study. Taylor et al. (1980) noticed that faults are commonly mapped as a single continuous line. This study showed that faults are more complex than is often implied by this mapping style. In Portola Valley they found a pattern of en echelon faulting and ground warping that had occurred during the 1906 event. They concluded that surface rupture in 1906 was transferred from the Woodside trace to the Trancos trace in a left-stepping en echelon behavior. They argued that surficial strain transfer between the two en echelon traces was accomplished by compressive buckling recorded by the warping of beds and ground surface in the overlap zone.

More recent studies have debated whether or not the Trancos trace experienced offset during the 1906 event (Wright et al., 2001). Subsequent investigations have shown Holocene slip, but not unequivocally 1906 activity (Fisher et al., 2002).

San Andreas Dam Investigation

In 1979 and 1981, N.T. Hall assisted in an investigation of the seismic safety of San Andreas Dam (Fig. 3). The study focused on the likelihood of a repeat 1906-type event. The San Francisco Public Utilities Commission wanted to know where and when the next large earthquake on the SAF was going to occur and if the San Andreas Dam was in danger of failure.

Hall found only one trace of the SAF, and it offset the rock in the left abutment but not the dam embankment. He concluded that the dam would sustain minimal damage if another large 1906-type earthquake were to occur. According to Hall's estimate, five 1906-magnitude events occurred within the last 1130 ±160 years. He interpreted that the SAF at San Andreas Dam has an average recurrence interval of 224 ± 25 years for 1906-type events.

Hall also noted that gouge along a fault trace is not always susceptible to erosion. The gouge encountered at San Andreas Dam is composed of Franciscan mélange bound together by hard plastic clay. In this case the gouge is more resistant to erosion than the highly fractured greenstone and greywacke adjacent to the active trace.

Filoli Center

About 13 kilometers northwest of the town of Portola Valley, Hall et al. (1999) performed an extensive paleoseismic study along the SAF at the Filoli Center. Here, Spring Creek has created an alluvial fan across the 1906 rupture trace of the SAF. Offset stream channel thalwegs were used as piercing points to document offset events. Hundreds of meters of trench wall were logged as the trenches were systematically excavated closer to the active zone of faulting (Hall et al., 1999). This technique allowed them to follow the piercing point to the fault trace.

From the data collected at the Filoli Center, they concluded that the SAP experiences two types of earthquakes, large 1906-type events that rupture four segments of the northern SAF, and smaller 1838-type events that rupture only the SAP. By their calculations, the SAP experiences a slip rate of 17 ± 4 mm yr^{-1}.

Portola Valley Town Center Investigation

In January 2004, William Lettis and Associates submitted a surface-fault rupture hazard evaluation to the town of Portola Valley. The purpose of their study was to assess the potential for surface fault rupture across the Portola Valley Town Center property, and to develop appropriate setbacks from active faulting and folding for the proposed New Town Center. The State of California Alquist-Priolo Earthquake Fault Zone Map shows three traces of the SAF crossing the Town Center property. Only two of these traces, the Woodside Trace and the Trancos Trace, have been documented in exploratory trenches. The third was mapped based on a lineament observed in aerial photographs. As part of the William Lettis and Associates investigation, a total of approximately 142 meters of trench wall were logged from both sides of two trenches to evaluate secondary faulting or folding off of the main active trace of the SAF (the Woodside trace).

William Lettis and Associates concluded that there was no evidence for faulting within the depth that was explored. Because of the high water table, the trenches were limited to about 3.5 meters deep, and the oldest material dated was 1,200 years old.

GEOLOGIC INVESTIGATION

Site Selection

With its linear shape and numerous sag ponds, it should be obvious that Portola Valley is a fault feature. The valley offers several advantages for conducting a paleoseismic study. The steep slopes of the Santa Cruz Mountains to the west and the accompanying drainage channels provide ample sedimentation to the valley. The large amounts of sediment and rapid subsidence (Hall et al., 2001) provide a thick sequence of Holocene deposits that preserve a detailed record of faulting activity in the valley.

Trench locations in Portola Valley were chosen based on several factors, one of which was permission to trench on private land. Many homeowners do not want the inconvenience of an open trench on their property for several weeks to several months. Fortunately the Town of Portola Valley already experienced trenching activities on their property for the New Town Center investigation and was generous enough to allow additional trenching activities on their property for research.

Trench T2 is located as close as possible to the 1906 en echelon fractures in Portola Road (Figs. 8 and 14), without trenching in the road. Fortunately a photo was taken shortly after the 1906 Earthquake preserving a record of surface rupture at the site. This photographic record was used to select a specific trenching site, essentially guaranteeing that the fault would be found, because it marked the location where the fault had previously ruptured (Fig. 13). Figure 13 shows a comparison of the site in 1906 and 2006.

Stratigraphy

The stratigraphic units mapped in Portola Valley consist of the Whiskey Hill Formation, the Monterey Formation, the Purisima Formation, the Santa Clara Formation, and older aluvial fan deposits. The geologic map by Brabb et al. (2000) shows the Whiskey Hill Formation and older alluvial fan deposits at the site of trench T2. During the investigation in trench T2, a poorly consolidated sandstone overlain by interbedded Holocene fluvial and marsh deposits (Plates 2 and 3) was observed. In Trench T1, only the interbedded Holocene fluvial and marsh deposits were observed. A detailed description of each individual lithologic unit is presented in Table 1.

Figure 13. Portola Road in 1906 and 2006. These photographs show what it looked like shortly after the earthquake of April 18, 1906 (top) and what it looked like in 2006 (bottom). The photo on the bottom was taken on February 8, 2006 looking S10E from the porch of the same house from which the 1906 photo was taken. The only objects in the 1906 photo that remain the same today are the road and the mountains in the background; both are obscured by vegetation. 1906 photo from the Stanford University Archives, J.C. Branner Collection, courtesy of the U.S. Geological Survey.

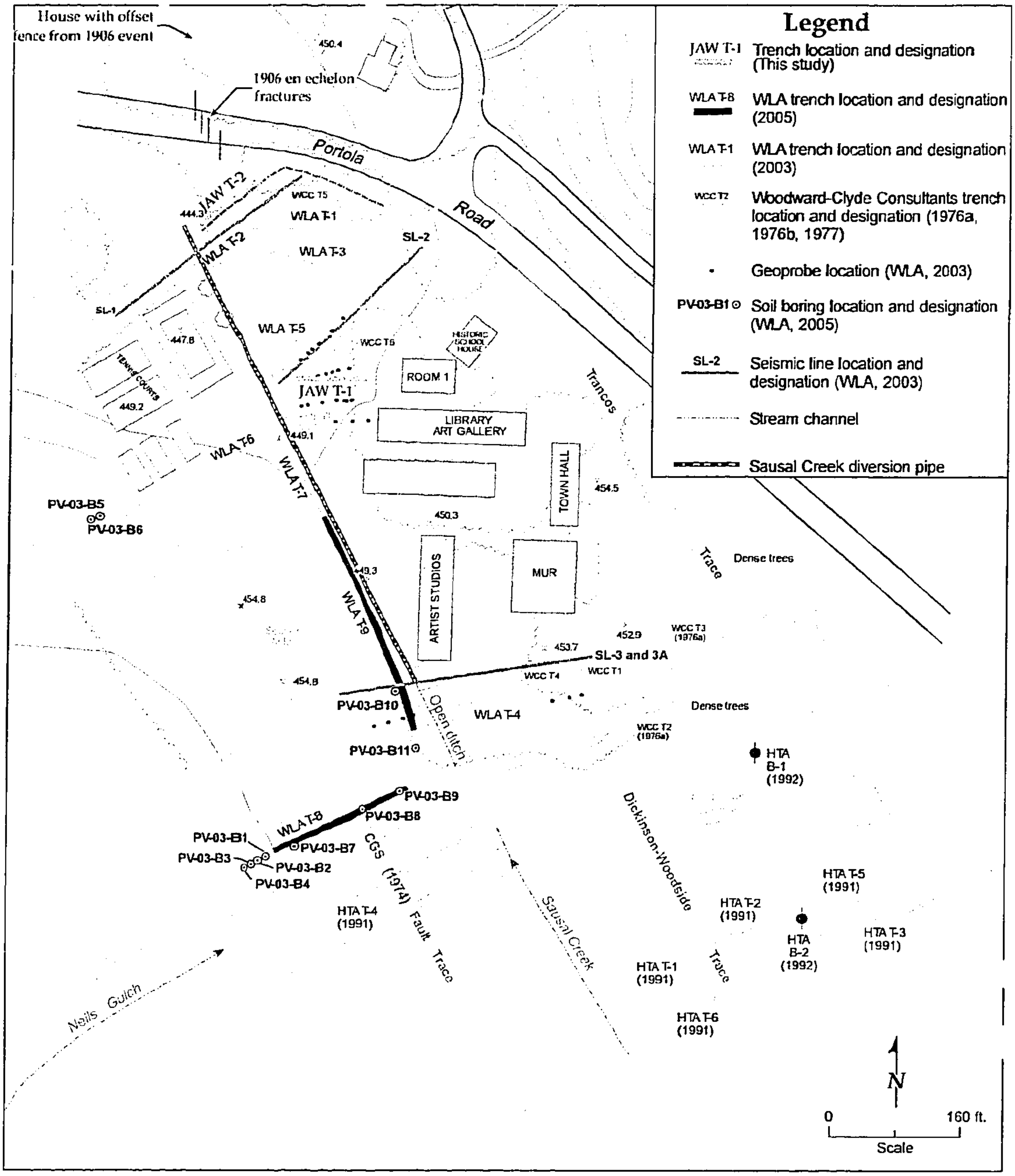

Figure 14. Subsurface Exploration Location Map. This map shows the locations of trenches, soil borings, geoprobes and seismic refraction surveys of the several seismological studies conducted at and near the project site. Modified from William Lettis and Associates, 2004.

Table 1. Unit descriptions as numbered on Plates 2 and 3 (trench logs).

Unit	Composition	Description
West of the fault zone (youngest to oldest)		
135	Brown to light yellow-brown sandy gravel to gravely silt	Bedded with clasts <0.5 cm, rounded with granular matrix. Slightly silty sand overbank, massive, clearly and abruptly cuts into underlying unit.
130	Pale brown sandy silt	Occasional light orange clast <0.5cm. Bioturbated with rootlets. Plastic found in this unit.
120	Dark brown to gray-brown clayey silt to silty clay	Large to medium blocky peds, massive. Gradual basal contact, marsh deposit.
115	Pale brown to light brown silty sand to sandy silt	Massive, friable, faint FeO_2 mottles, rootlets, overbank deposit.
110	Brown to dark brown sandy gravel to gravelly sand	Imbricated pebbles, massive to bedded layers undulating and interfingering with tan silty sand.
105	Brown to dark yellow-brown sandy silt	Faint horizontal bedding, strongly mottled.
100	Dark to olive-brown clayey silt	Zones of brown silty mottles, abundant charcoal, gradual basal contact.
95	Dark brown sandy clay	Massive, abundant charcoal, clear basal contact. Marsh deposit.
90	Tan to light yellow-brown silt to fine sand	Firm to soft, mottled, clear basal contact with some undulations.
88	Dark yellow-brown clayey silt to silty clay	Massive overbank deposit, zones of oxidation, trace sand.

Unit	Composition	Description
85	Yellow clayey silt with sand	Strongly oxidized, massive, reduced zones, clear to gradual basal contact.
80	Yellow to olive-brown clayey silt to silty clay	Massive, abundant charcoal, very diffuse basal contact, marsh deposit.
70	Yellow-brown clayey silt with sand	Faint orange oxidation mottles, massive, abundant charcoal at base, sharp basal contact. Overbank deposit.
60	Black to dark gray silty clay	Massive, brown silty mottles, abundant charcoal, clear basal contact. Marsh deposit.
50	Dark brown to dark yellow-brown silty clay	Massive with trace fine sand, orange-brown oxidation mottles, diffuse basal contact.
40	Dark gray-brown to gray-black silty clay	Massive, occasional gray reduced zones, diffuse to gradual contact.
35	Dark brown silty clay	Massive with trace fine sand, trace faint dark orange-brown mottles, reduced zones.
30	Dark gray clayey sand	Fine sand with coarse sand clasts, massive, wavy to smooth lower boundary.
25	Gray-brown silty sand	Fine grained sand, massive.
Within and east of the fault zone (youngest to oldest)		
6	Tan to light brown silty clay to clayey silt	Massive, unclear contacts, abundant rootlets.
5	Light brown silty clay to clayey silt	Strongly oxidized, fine $CaCO_3$ nodules.
4	Brown silty clay	Massive, unclear contacts, abundant rootlets.

Unit	Composition	Description
3	Tan to light brown silty sand	Hard, mottled with oxidized blotches, fine $CaCO_3$ nodules, white siltstone clasts.
2	Dark brown clay	Trace sand and gravel, few $CaCO_3$ nodules.
1	Light olive-brown clay with sand	Contains large (1-2 cm diameter) $CaCO_3$ nodules.

Whiskey Hill Formation

The Whiskey Hill Formation is described by Brabb et al. (2000) as a light-gray to buff coarse-grained arkosic sandstone, with light-gray to buff silty claystone, glauconitic sandstone, and tuffaceous siltstone. Multiple fault planes were identified within the Whiskey Hill Formation and their orientations are presented in Table 2.

Table 2. Fault orientations within the Whiskey Hill Formation.

Fault No.	Strike	Dip
1	N65W	90°
2	N75W	88° SW
3	N6E	90°
4	N31W	90°
5	N61W	80° SW
6	N65W	85° SW
7	N8W	88° NE
8	N10W	80° NE
9	N18W	82° NE
10	N16W	80° NE
11	N40W	90°
12	N16W	80° NE
13	N18W	74° NE
14	N38W	80° NE
15	N25W	75° NE
16	N15W	78° NE

Trenching Investigation

Two trenches (Fig. 14), each about 13 meters long by 2 .5 meters deep, were excavated in the town of Portola Valley on October 10, 2005 by a tire-mounted backhoe equipped with a 1-meter-wide bucket. Trench T1 was located between the baseball field and the basketball courts on the Portola Valley Town Center property, and oriented approximately N79W. Trench T2 was located between the Town Center baseball field and the roadside parking lot for the Christ Episcopal Church, and was oriented approximately N39E.

The trenches were excavated and shored, and the trench walls were scraped clean and smooth to provide an enhanced view of the stratigraphy and the structural relationships of the layers. Following the cleaning of the walls of the trenches, a grid was set up on each trench wall using string held in place by nails. The bottom of each stratigraphic unit was marked with a different colored flag (tape) for each unit. Detailed logs of both trenches were made for each trench wall at a scale of 1 inch = ½ meter (Plates 1 and 2). The logs provide a detailed record of what was observed on the trench walls.

In trench T1, no faulting or folding was observed. In trench T2 (Plates 1 and 2) faulting was found in the east end of the trench on both the north and south walls. The majority of the faults occur in a thick-bedded unit (interpreted as belonging to the Whiskey Hill Formation) at the east end of the trench. There was insufficient evidence, however, to confirm that any of these faults extended to the 1906 ground surface. The Whiskey Hill Formation, through which the faults cut, contained no dateable material. For these reasons the faulting observed in the Whiskey Hill Formation provided very little information on the timing of surface rupture events.

Several colluvial wedges were observed on the west side of the fault zone, which indicate a west-facing scarp. Two and possibly three colluvial wedges were identified on the north wall of trench T2; on the south wall of trench T2, no differentiation could be made between the lower two wedges.

Samples of detrital charcoal were collected to determine ages of the stratigraphic units and colluvial wedges, and their locations were recorded on the logs. Historical artifacts, such as wire, nails, and pottery were noted and their positions on the walls of the trenches were recorded on the logs.

Radiocarbon Dating

Many of the alluvial deposits in Portola Valley contain abundant detrital charcoal which was used in dating some of the stratigraphic units. Fourteen charcoal samples were dated by radiocarbon analysis using the accelerator mass spectrometry (AMS) method at the Lawrence Livermore National Laboratory (LLNL) in Livermore, California and the NSF-Arizona Accelerator Mass Spectrometry facility in Tucson, Arizona. The laboratory results were calibrated to calendar years using the computer program CALIB revision 5.0.1 (Stuiver and

Reimer, 2004). The locations of the dated charcoal samples are shown on the trench logs (Plates 1 and 2).

The samples range in age from 40 BC to 1950 AD. Table 3 contains the calibrated age ranges of each of the dated samples. The ages of the same units on opposing trench walls generally agree. The only discrepancy in ages was from sample 6S, which was found to be much older than the four other samples from the same unit. This anomalously old age may indicate transport and redeposition of pre-existing charcoal in a younger stratigraphic unit. This means that each of the ages is a maximum age, and that the lithologic units can be younger than suggested by the radiocarbon ages.

Table 3. Radiocarbon dates of detrital charcoal samples.

Sample Number	Stratigraphic Unit	$\delta^{13}C$	^{14}C Age, yr B.P.	Calendar Date A.D. (probability)
PV-T2-RC-30N	6	-28.8	625±35	1290-1400 (1.00)
PV-T2-RC-36N	6	-25	715±35	1230-1310 (.886) 1360-1390 (.114)
PV-T2-RC-9S	6	-25	585±35	1300-1370 (.681) 1380-1420 (.319)
PV-T2-RC-7S	6	-25	690±35	1260-1320 (.683) 1350-1390 (.317)
PV-T2-RC-6S	6	-26.1	1665±35	260-300 (.111) 320-440 (.847) 490-510 (.027) 520-530 (.015)
PV-T2-RC-19N	40	-24.8	1965±35	40 BC-90 AD (.955) 100-120 (.045)
PV-T2-RC-18N	60	-24.9	900±45	1030-1220 (1.00)
PV-T2-RC-25N	80	-24.4	695±35	1260-1320 (.720) 1350-1390 (.230)
PV-T2-RC-22N	100	-26.8	465±40	1330-1340 (.001) 1400-1490 (.987) 1600-1610 (.012)
PV-T2-RC-3S	120	-25	397±31	1440-1520 (.770) 1560-1560 (.001) 1570-1630 (.229)
PV-T2-RC-33N	120	-25	375±45	1440-1530 (.536) 1540-1640 (.464)
PV-T2-RC-34N	130	-26.3	220±35	1530-1540 (.006) 1640-1690 (.376) 1730-1810 (.482) 1925-1950 (.135)
PV-T2-RC-12N	Wedge Y	-25.8	2195±40	380 BC-170 BC (1.00)
PV-T2-RC-2N	Wedge Z	-25	665±35	1270-1330 (.519) 1340-1390 (.481)

RECURRENCE INTERVAL

A recurrence interval is the average time between events. For this study the events that are under consideration are large surface-rupturing earthquakes. Currently, the USGS estimates an average recurrence interval of approximately 225 years for the SAP (Bryant and Lundberg, 2003). 1906-type earthquakes that rupture all of the northern California SAF fault segments are believed to occur every 180 to 370 years (WGCEP, 2003).

The recurrence interval of a fault is required for calculating probability of rupture on that fault. Recurrence interval data obtained from the paleoseismic record provide important checks of recurrence intervals resulting from earthquake models (WGCEP, 2003).

Portola Valley Site Findings

Although dateable offset features were not encountered in the trenches explored for this study, several colluvial wedges were observed, all indicating a west-facing scarp (Plates 1 and 2). Although the SAF is a strike-slip fault, the 1906 event did have a vertical component of slip. Lawson wrote:

> The differential displacement of the earth's crust effected by the movement on the San Andreas fault on April 18, 1906, may for convenience be resolved into two components, the horizontal and the vertical. The vertical movement was small compared with the horizontal, was quite variable and ranged from a few inches up to about 3 feet. (Lawson, 1908)

It is reasonable to conclude that previous surface-rupturing earthquakes could have formed small scarps at the site capable of producing colluvial wedges such as those encountered in exploratory trench T2 (Plates 1 and 2). By constraining the ages of the colluvial wedges, we can estimate the recurrence interval for large surface rupturing events such as the 1906 event.

The most recent, wedge X, overlies unit 120, wedge Y, and unit 6. It is situated below a stream channel deposit, unit 130, and the uppermost (modern) soil unit (Plates 1 and 2). The wedge is composed of mottled brown sandy silt. It contains fragments of siltstone similar to the bedrock siltstone units (i.e., unit 6) to the east, within the fault zone. The siltstone would have been located within the scarp face, so it seems reasonable that fragments would be found in the colluvium. Radiocarbon dating shows that this unit is younger than A.D. 1440 (unit 120, sample 33N) and the presence of historical artifacts makes wedge X younger than the mid 19th century. The plastic found near the bottom of unit 130 is consistent with my interpretation that the 1906 ground surface is at the top of unit 120.

The estimated average sedimentation rate in Portola Valley is 4.0 to 4.4 mm per year (Hall et al., 2001). According to Hall et al. (2001), this "suggests relatively rapid subsidence and concurrent sedimentation within the Portola Valley basin throughout the Holocene." This rate would place the 1906 ground surface at or just above the top of unit 120. It is likely that wedge X represents the colluvial wedge developed from the scarp created by the 1906 surface rupture event. A piece of milled wood found within wedge X provides additional support for this view.

Like wedge X, wedge Y is composed of brown clayey sandy silt and contains siltstone fragments. Wedges Y and Z are very close in age, and therefore could represent a single colluvial event, wedge Y-Z. Assuming a single wedge, Y-Z, the earthquake that produced the scarp from which the wedge was formed would have occurred after 1325 ± 65 (unit 80, sample 25N). However, the logs show the combined wedge Y-Z in different stratigraphic locations on either side of the trench, suggesting that perhaps evidence for the existence of wedge Z is missing or obscured on the south wall.

The argument can be made that wedge Y is younger than the detrital charcoal samples suggest, for reasons explained above. If wedges Y and Z represent separate events, then wedge Z would have formed concurrent with unit 100, meaning the earthquake responsible for triggering the formation of wedge Z occurred before 1445 ± 45 (sample 22N).

An additional date of a large surface rupturing event can be obtained from the tilting of the fluvial deposits. Units 60 and below are tilted down to the southwest. The units above unit 60 are relatively horizontal, indicating that a faulting event large enough to tilt these layers occurred after the deposition of unit 60, after 1125 ± 95 (sample 18N) and before the deposition of unit 70 (sample 25N, 1285 ± 15). It is possible, however, that units 70, 80, and 85 were deposited before the tilting event occurred and were truncated by erosion prior to the deposition of unit 88. In this case, the upper bound of the tilting event would be 1445 ± 45 (sample 22N).

Therefore, if there are three colluvial wedges and one tilting event between 1030 and 1906, then a recurrence interval of 292 years can be calculated. This is done by calculating the maximum total number of years between the first and the last events divided by the number of time intervals between events. An average maximum recurrence interval of 438 years between surface rupturing events can be calculated if there are only two colluvial wedges and a tilting event.

Discussion

Results/Implications

This investigation shows that multiple surface faulting events occurred on the SAP prior to the 1906 event. The penultimate event on the SAP, as indicated by the data collected at this site, occurred between 1445 ± 45 (sample 22N) and 1540 ± 100 (sample 33N) A.D. if wedges Y and Z represent two separate events. The exact number of events that occurred at this study site is uncertain due to the differing north and south wall logs, and to the uncertainty of how any colluvial wedges are present. One of the reasons for the difference could be because the south wall did not dry completely. The south wall was located adjacent to the

Portola Valley Town Center baseball field. The baseball field was watered several times while the trench was open, preventing the wall from drying adequately. Hall et al. (2001) suggested as a minimum guideline to trenching investigations that "trenches in clayey soils should be kept open several days or long enough to allow the walls to dry sufficiently to reveal hidden shears." The area beneath wedge X in particular remained obscured by the moisture and made it difficult to differentiate between lithologic units. For this reason, the author favors the three-wedge conclusion and recurrence interval of 292 years.

Taking into consideration possible redeposition of charcoal, the dates that were obtained do not firmly constrain upper limits on ages of events, and therefore make interpretation difficult without making assumptions. Based on the dated material, there is a long period of time (360 years) between the tilting of unit 60 and the deposition of wedge Z. This leads one to consider that perhaps one or more surface rupture events are missing from the record in this trench site. One possibility is that faulting occurred east of the excavation, and was not seen in the trench. Another possibility is that faulting occurred on the Trancos trace of the SAF. If we assume that at least one event is missing from the record between the tilting event and the 1906 event, then the three- and two-wedge recurrence intervals would be 219 and 292 years, respectively.

Comparison with prior studies

Hall (1984) estimated a recurrence interval of 224 ± 25 years for the SAP. He first calculated a slip rate using radiocarbon dating of alluvium incised into an offset stream. Using this slip rate, his recurrence interval estimate was then based on the 2.7 meters of offset observed during the 1906 event and the number of 2.7-meter-offset events required to straighten out an offset stream. Hall's recurrence interval of 225 years closely matches the recurrence intervals calculated here, using three wedges. Hall's estimate however, could be erroneous if 2.7 meters is not an accurate average offset distance for prehistoric surface rupture events on the SAP, or if his radiocarbon age does not reflect the true age of the stream incision.

Previous paleoseismic studies on the SAF have attempted to identify the penultimate 1906-type earthquake (Schwartz et al., 1998 and Hall et al., 1999). The timing of the penultimate event from multiple trench studies in the North Coast, Peninsula, and Santa Cruz Mountains segments of the SAF (Table 4) has been compared to narrow the range of time during which it could have occurred. See Figure 2 for mapped locations of these sites.

Table 4. Estimated penultimate event on the northern section of the SAF.

PENULTIMATE EVENT DATA

Segment	Site Name	Reference	Estimated Penultimate Event Date
North Coast	Point Arena	Prentice, 1989	After 1530 A.D.
	Vedanta	Niemi, 1992 and Niemi and Hall, 1992	After 1588
	Dogtown	Niemi, 1992	After 1521
Peninsula	Filoli	Hall et al., 1999	After 1450
	Portola Valley	This Study	After 1400
Santa Cruz Mountains	Grizzly Flat	Schwartz et al., 1998	Before 1665
	Coward Creek	Heingartner and Schwartz, 1996	Before 1669 and After 1431

The assumption is made that each of these penultimate events represents a 1906-type event where all three fault segments of the SAF rupture at the same time.

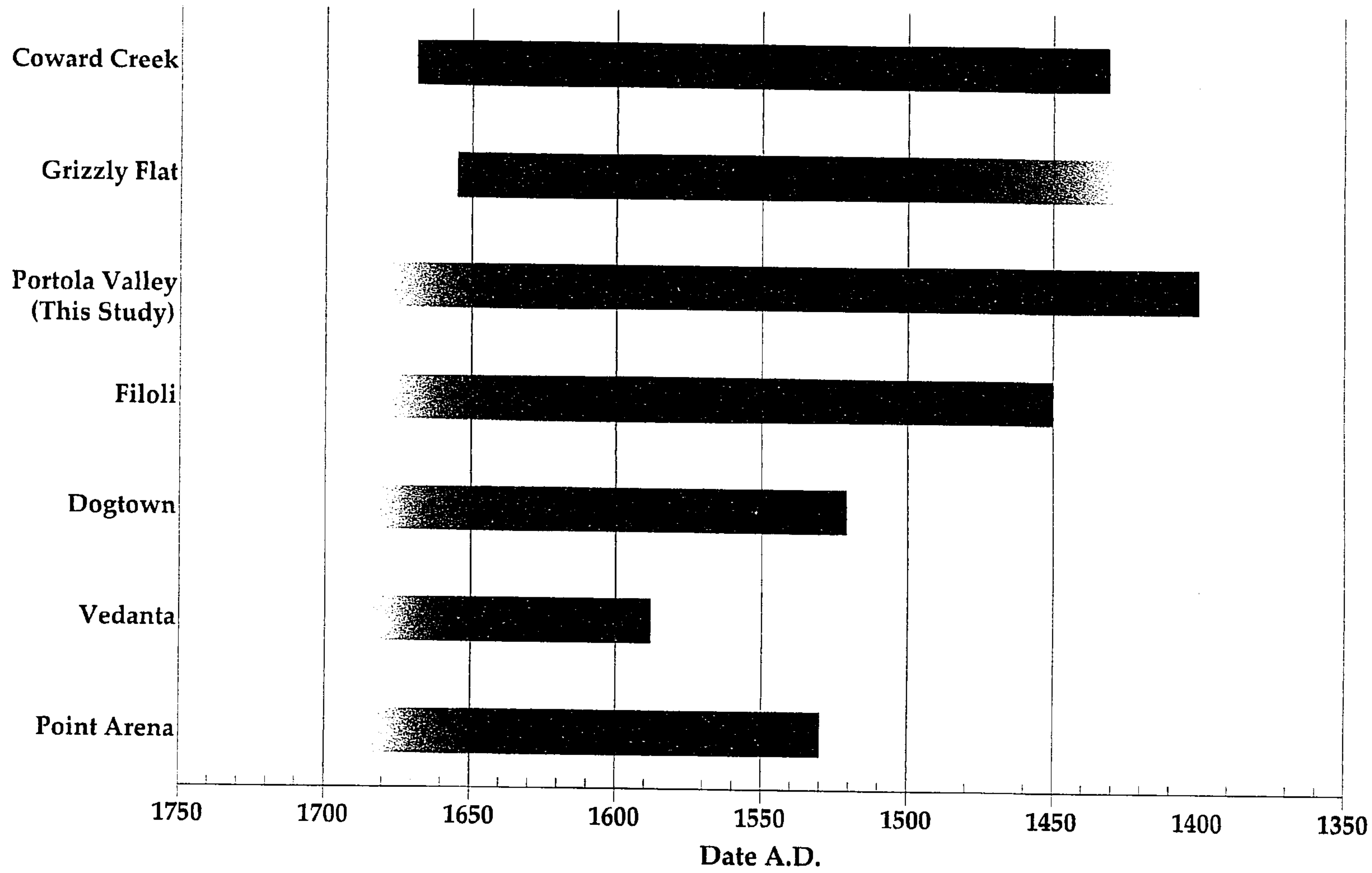

Figure 15. Penultimate Surface Rupturing Events on the San Andreas Fault. These records show that a large earthquake rupturing at least three fault segments probably occurred on the SAF sometime between 1655 and 1588 A.D. Unconstrained upper and lower bounds fade to white.

Figure 15 shows a diagram, modeled after Hall et al. (1999), that includes the data from this study and previous studies on the northern section of the SAF. The event timing calculated from this study matches with previous work that the penultimate 1906-type event occurred between 1665 and 1588.

Uncertainties

In scientific analysis, uncertainties are generated where assumptions are made. In a paleoseismic study these assumptions include, among others, the assumption that detrital charcoal is not reworked, and human error. Whereas these are accepted sources of uncertainty by most in the geologic community, other uncertainties exist in this analysis that all may not agree upon. The following is a discussion regarding the known uncertainties and assumptions made in this analysis.

Figure 8 is a reproduction of a photograph taken near trench T-2 shortly after the April 18, 1906 event. The en echelon fractures are clearly visible in the photograph; however, a scarp is not evident. Although it is not impossible, it is hard to comprehend how such a negligible scarp could produce the size of colluvial wedge recorded on the trench logs. One explanation is that the wedge could have been disturbed and lengthened as a result of the tilling of the land, as it was located in a plum orchard. Another possibility is that wedge X could represent a combined 1906/1838 colluvial wedge. It is unknown if the 1838 earthquake produced surface rupture in the Portola Valley area.

During the excavation of trench T-2, a French drain was encountered and removed. As seen on the west side of Plate 2, a layer of gravel remained on the trench wall after the completion of the excavation. During the process of cleaning the trench walls for analysis, the gravel nearest the fault zone was removed. Every effort was made to clean the walls properly and remove all foreign material that was placed during the installation of the French drain. It is possible that the plastic found in unit 130 came from the French drain and was not deposited with unit 130 thus, possibly changing the location of the interpreted 1906 ground surface.

Plate 2 shows the location of the piece of milled wood at the bottom of wedge X. Certainly, to all of those who saw its location in the field, it was located at the bottom of wedge X. However, it is possible that it could have come from the stream channel deposit. Both the milled wood and the plastic provide compelling evidence for the conclusion that unit 130 was deposited after 1906.

Without these pieces of evidence, only the radiocarbon dates can provide an age of unit 130, and in turn, wedge X. Unit 130 would range in age between 1530 and 1950 A.D.

Finally, as previously discussed, other surface rupture events could have occurred without producing a scarp. A slip event with little or no vertical component could have occurred without leaving behind evidence of its happening. Despite these uncertainties, it is the author's opinion that the results of this study are the most credible.

CONCLUSIONS

Analysis of paleoseismic data from trenches in Portola Valley, California provides insight into the behavior of the Peninsula segment of the San Andreas fault. Trenching revealed fault-derived colluvial wedges that provide event timing for large 1906-type surface rupture earthquake events. The radiocarbon dating of fluvial strata and the colluvial wedges indicates possible recurrence intervals of 292 and 438 years on the SAP for three- and two-wedge scenarios, respectively. The number of colluvial wedges is uncertain because the logs of the north and south walls of trench T2 do not match (Plates 1 and 2). One reason the logs do not match could be because the south wall did not dry at the same rate as the north wall and obscured some of the lithologic contacts. For this reason, the author favors the three-wedge option inferred from the north wall of the trench.

The date of the penultimate event recorded on the trench logs for this investigation is post-1400 A.D. Radiocarbon dating did not allow for an upper bound on the timing of this event. However, this date matches previous estimates by multiple authors of the penultimate 1906-type surface rupture event on the northern section of the SAF. The previous multi-segment earthquake on the northern section of the SAF, prior to 1906, is believed to have occurred between 1665 and 1588 (Fig. 14).

REFERENCES

Argus, D.F., and Gordon, R.G., 1991, Current Sierra Nevada–North America motion from very long baseline interferometry: Implications for the kinematics of the western United States: Geology, v. 19, p. 1085–1088.

Argus, D.F., and Gordon, R.G., 2001, Present tectonic motion across the Coast Ranges and San Andreas fault system in central California, GSA Bulletin, December 2001, v. 113, no. 12, p. 1580-1592.

Atwater, T., and Stock, J., 1998, Pacific-North American plate tectonics of the Neogene southwestern United States: An update, International Geology Review, v. 40, p. 375-402.

Bakun, W.H., 1999, Seismic activity of the San Francisco Bay region, Bulletin of the Seismological Society of America, v. 89, no. 3, p. 764-784.

Brabb, E.E., Graymer, R.W., and Jones, D.L.,2000, Geologic map and map database of the Palo Alto 30′ by 60′ quadrangle, California, scale 1:1,000,000

Bryant, W.A., and Lundberg, M., compilers, 2003, Fault number 1c, San Andreas fault zone, Peninsula section, *in* Quaternary fault and fold database of the United States: U.S. Geological website, http://earthquakes.usgs.gov/regional/qfaults, accessed at 03/03/2006 09:51 AM.

Clarke, S.H., Jr., and Nilsen, T.H., 1973, Displacement of Eocene stata and impilications for the history of offset along the San Andreas fault, central and northern California, *in* Kovach, R.L., and Nur, Amos, eds., Proceedings of the conference on tectonic problems of the San Andreas fault system: Stanford, California, Stanford University Publications in the Geological Sciences, v. 13, p. 358-367.

Davis, G.H., and Reynolds, S.J., 1996, Structural geology of rocks and regions, New York, John Wiley & Sons, Inc., p. 365-370.

Dickinson, W.R., 1970, Commentary and reconnaissance photogeologic map, San Andreas rift belt, Portola Valley, California: report to Town of Portola Valley Planning Commission, dated July 6, 1970.

Fisher, G.R., Anderson, P.C., and Stewart, C.S., 2002, Holocene activity of the Trancos trace, San Andreas fault, Portola Valley, San Mateo County, northern California, Geological Abstracts with Programs, v. 34, no. 5, p. 86.

Fumal, T.E., Heingartner, G.F., and Schwartz, D.P., 1999, Timing and slip of large earthquakes on the San Andreas fault, Santa Cruz Mountains, California: Geological Society of America Abstracts with Programs, v. 31, no. 6, p. A-56.

Hall, N.T., 1984, Holocene history of the San Andreas fault between Crystal Springs Reservoir and San Andreas Dam, San Mateo County, California, Bulletin of the Seismological Society of America, v. 74, no. 1, p. 281-299.

Hall, N.T., Wright, R.H., and Clahan, K.B., 1999, Paleoseismic studies of the San Francisco Peninsula segment of the San Andreas fault zone near Woodside, California, Journal of Geophysical Research, v. 104, no. B10, p. 23,215 - 23,236.

Hall, N.T., Wright, R.H., and Prentice, C.S., 2001, Studies along the peninsula segment of the San Andreas fault, San Mateo and Santa Clara Counties, California, *in* Ferriz, H. and Anderson, R., eds., Engineering Geology Practice in Northern California, CDMG Bulletin 210, p. 193 to 210.

Heingartner, G.F., and Schwartz, D.P., 1996, Paleoseismic evidence for large magnitude earthquakes along the San Andreas fault in the southern Santa Cruz Mountains, California, EOS Transcript, AGU, v. 77, no. 46, Fall meeting supplement, p. F462.

Irwin, W.P., 1990, Geology and plate-tectonic development, *in* Wallace, R.E., ed., The San Andreas fault system, California, U.S. Geological Survey professional paper 1515, Washington D. C., United States Government Printing Office, p. 61-80.

Kelson, K.I., Lettis, W.R., and Lisowski, M., 1992, Distribution of geologic slip and creep along faults in the San Francisco Bay Region, *in* Brochardt, G. et al., eds., Proceedings of the Second Conference on Earthquake Hazards in the Eastern San Francisco Bay Area: California Department of Conservation, Division of Mines and Geology Special Publication 113, p. 31-38.

Lawson, A.C., 1908, The earthquake of 1868; *in* Lawson, A.C., ed., the California earthquake of April 18, 1906: Report of the State Earthquake Investigation Commission, v. 1: Carnegie Institute of Washington Publication 87, p. 105-107, 434-448.

Niemi, T.M., 1992, Late-Holocene slip rate, prehistoric earthquakes, and Quaternary neotectonics of the northern San Andreas fault, Marin County, California: Stanford, California, Stanford University, Ph.D. dissertation, p. 199.

Niemi, T.M., and Hall, N.T., 1992, Late Holocene slip rate and recurrence of great earthquakes on the San Andreas fault in northern California, Geology, v. 20, p. 195-198.

Noller, J.S., Simpson, G.D., and Lightfoot, K., 1996, Paleoseismic and geoarchaeologic investigations of the northern San Andreas fault, Fort Ross, California, in National Earthquake Hazards Reduction Program, Summaries of technical reports: U.S. Geological Survey, National Earthquake Hazards Reduction Program External Research Program, Annual Project Summaries, v. 37, http://erp-web.er.usgs.gov/reports/annsum/vol37/nc/g2474.htm. *in* Bryant, W.A., and Lundberg, M.Matthew, compilers, 2003, Fault number 1b, San Andreas fault zone, North Coast Section, in Quaternary fault and fold database of the United States: U.S. Geological website, http://earthquakes.usgs.gov/regional/qfaults, accessed at 03/03/2006 01:59 PM.

Page, B.M., Coleman, R.G., and Thompson, G.A., 1998: Overview: Late Cenozoic tectonics of the central and southern Coast Ranges of California, *in*

Geological Society of America Bulletin: v. 110, no. 7, p. 846–876.

Pampeyan, E.H., 1995, Maps showing recently active fault breaks along the San Andreas fault from Mussel Rock to the Central Santa Cruz Mountains, California: U.S. Geological Survey Open-File Report 93-684.

Prentice, C.S., 1989, Earthquake geology of the northern San Andreas fault near Point Arena, California: Pasadena, California, California Institute of Technology, Ph.D. dissertation, p. 252.

Prentice, C.S., Merritts, D.J., Beutner, E., Bodin, P., Schill, A., and Muller, J., 1999, The northern San Andreas fault near Shelter Cove, California: Geological Society of America Bulletin, v. 111, no. 4, p. 512-523.

Prentice, C.S., 1999, San Andreas fault: The 1906 earthquake and subsequent evolution of ideas, *in* Moores, E.M., Sloan, D., and Stout, D.L., eds., Classic Cordilleran Concepts: A View from California: Boulder, Colorado, Geological Society of America Special Paper 338, p. 69-85.

Schwartz, D.P., Pantosti, D., Okumura, K., Powers, T.J., and Hamilton, J.C., 1998, Paleoseismic investigations in the Santa Cruz mountains, California: Implications for recurrence of large-magnitude earthquakes on the San Andreas fault, Journal of Geophysical Research, v. 103, no. B8, p. 17,985-18,001.

Sarna-Wojcicki, A.M., 1992, Long-term displacement rates of the San Andreas fault system in northern California from the 6-Ma Roblar tuff [abs.], *in* Borchardt, Glenn et al., eds., Proceedings of the Second Conference on Earthquake Hazards in the Eastern San Francisco Bay Area: California Department of Conservation, Division of Mines and Geology Special Publication 113, p. 29-30.

Stuiver, M., Reimer, P. J., and Reimer, R. W. 2005, CALIB 5.0 WWW program and documentation, http://calib.qub.ac.uk/calib/.

Taylor, C.L., Cummings, J.C., and Ridley, A.P., 1980, Discontinuous en echelon faulting and ground warping Portola Valley, California, *in* Streitz, R., and

Sherburne, R., eds., 1980, Studies of the San Andreas fault zone in Northern California: Special Report 140, California Division of Mines and Geology, p. 59-70.

Toppozada, T.R., 2000, San Andreas $M \geq 5.5$ earthquakes from Parkfield to Fort Bragg, California, 1800-1999, *in* Proceedings, Third Conference on Tectonic Problems of the San Andreas Fault System, Stanford University, September 6-8, 2000, v. 1, p. 93-105.

Toppozada, T.R., Branum, D.M., Reichle, M.S., and Hallstrom, C.L., 2002, San Andreas fault zone, California: $M \geq 5.5$ earthquake history, Bulletin of the Seismological Society of America, v. 92, no. 7, p. 2555-2601.

Wakabayashi, J., 1999, Distribution of displacement on and evolution of a young transform fault system: The northern San Andreas fault system, California, Tectonics, v. 18, no. 6, p. 1245-1274.

Wallace, R.E., 1990, Geomorphic expression, *in* Wallace, R.E., ed., The San Andreas fault system, California, U.S. Geological Survey professional paper 1515, Washington D. C., United States Government Printing Office, p. 15-21.

William Lettis and Associates, Inc., 2004, Supplemental surface-fault rupture hazard evaluation, proposed Portola Valley Town Center, 765 Portola Road, Portola Valley, California, California Geological Survey Open-File Report AP-3230.

Working Group on California Earthquake Probabilities, 2003, Earthquake probabilities in the San Francisco Bay Region: 2002-2031: U.S. Geological Survey Open-File Report 03-214.

Wright, R.H., Crampton, T.A., and Hall, N.T., 2001, Paleoseismic Investigation of the San Andreas fault zone in Portola Valley, San Mateo County, California: Geomatrix Consultants, Inc., Oakland, California, NEHRP Element II, Award no. 01HQGR0009.

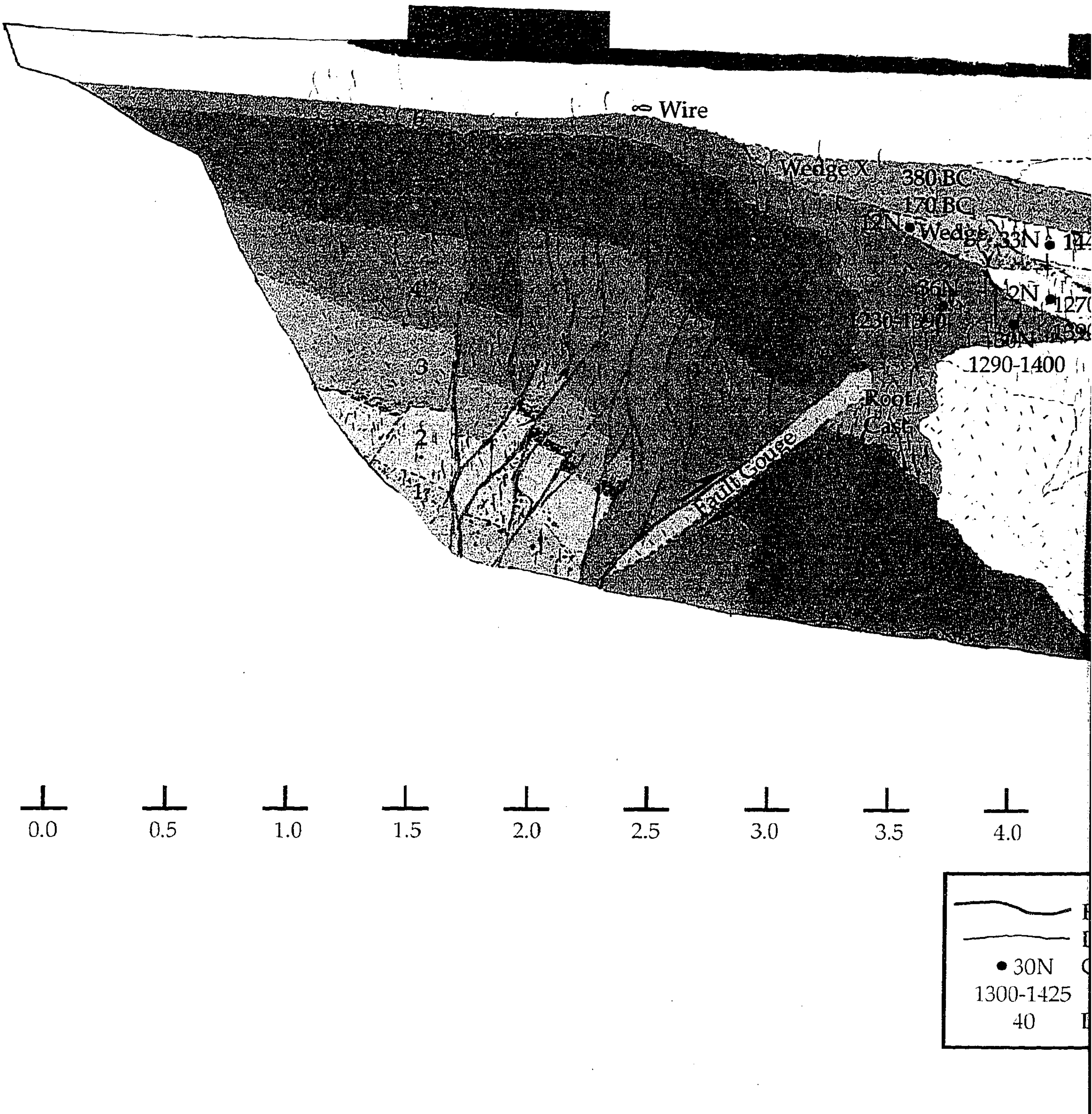

Wire
Wedge X
380 BC
170 BC
12N
Wedge
33N
36N
1230-1390
1290-1400
Root
Cast
Fault Gouge
4
3
2
1
0.0
0.5
1.0
1.5
2.0
2.5
3.0
3.5
4.0
30N
1300-1425
40

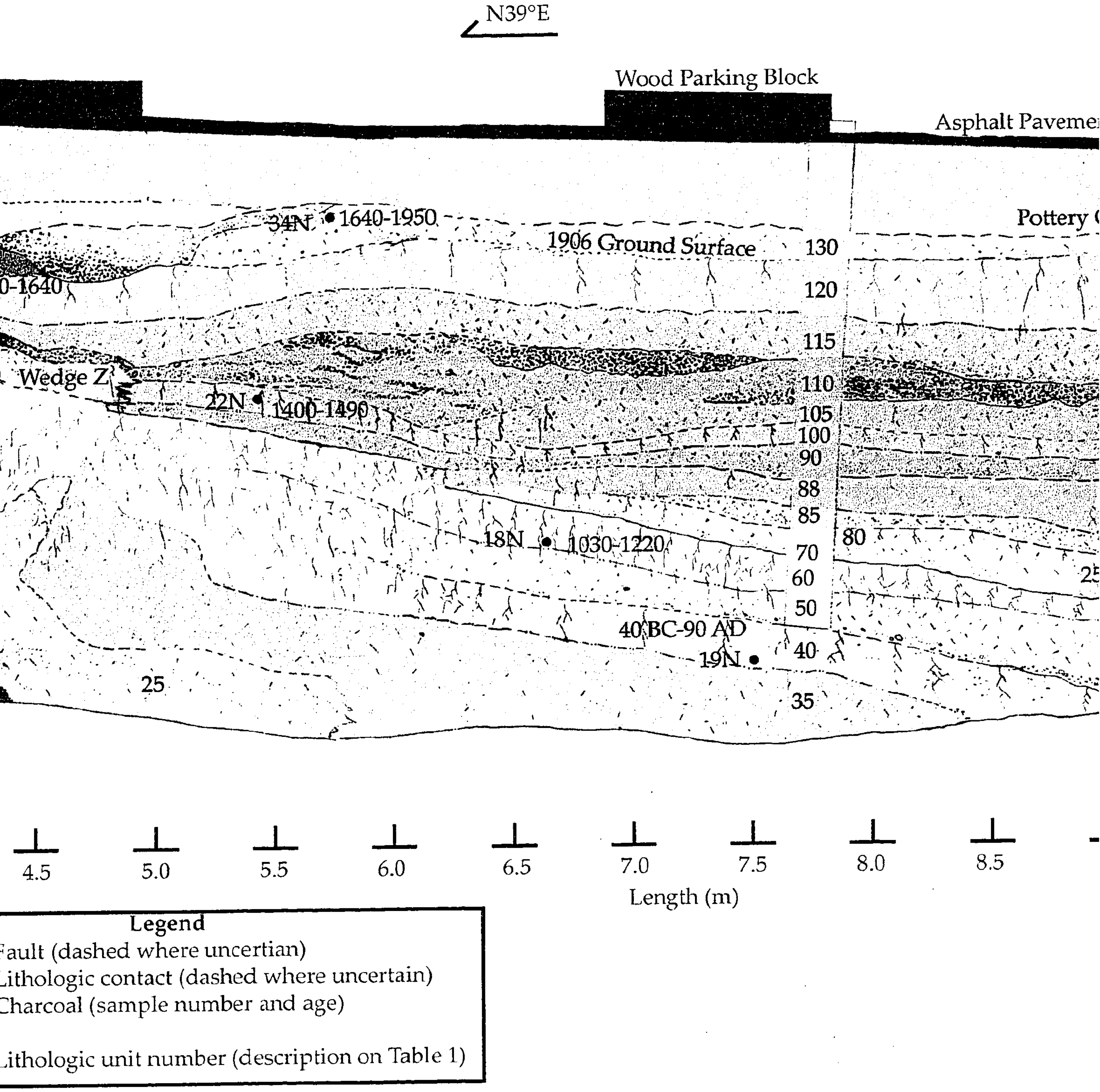

N39°E
Wood Parking Block
Asphalt Paveme
Pottery
34N
1640-1950
1906 Ground Surface
0-1640
Wedge Z
22N
1400-1490
18N
1030-1220
40 BC-90 AD
19N
130
120
115
110
105
100
90
88
85
80
70
60
50
40
35
25
4.5
5.0
5.5
6.0
6.5
7.0
7.5
8.0
8.5
Length (m)
Legend
Fault (dashed where uncertian)
Lithologic contact (dashed where uncertain)
Charcoal (sample number and age)
Lithologic unit number (description on Table 1)

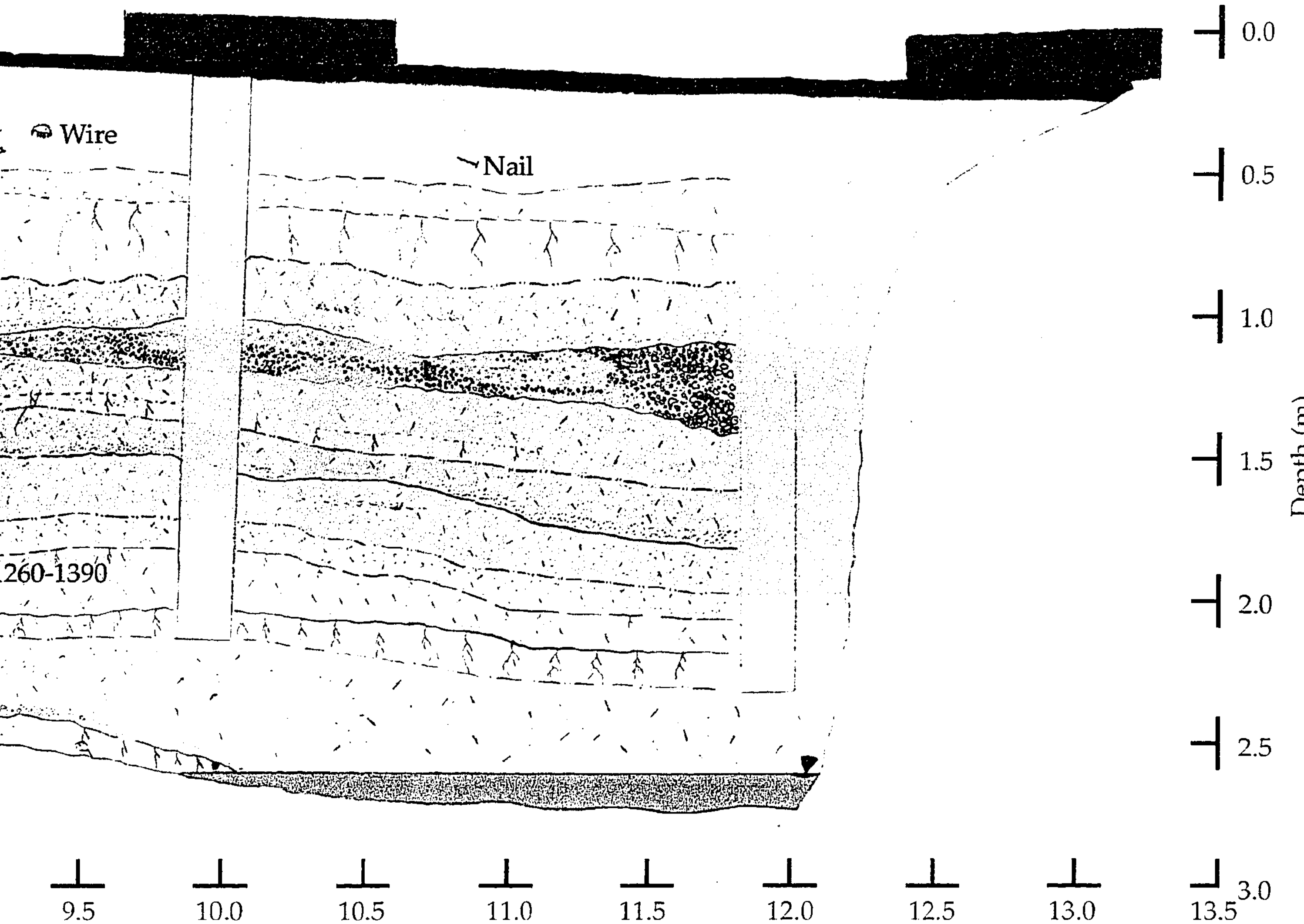

Plate 1. Inverted Log of North Wall of Trench T2.

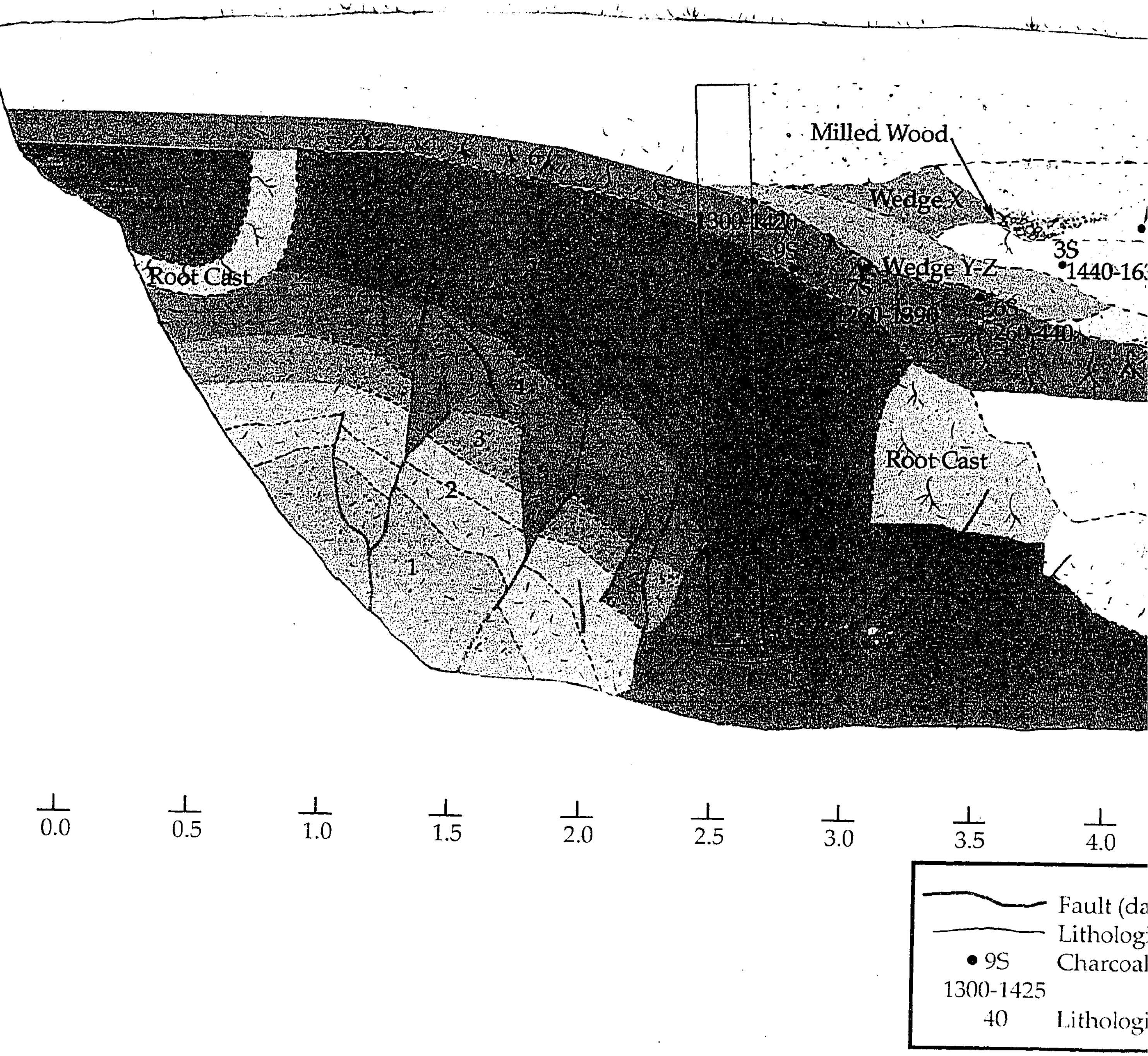

Milled Wood
Wedge X
Wedge Y-Z
3S
1440-163
9S
1300-1420
260-1390
26S
260-1410
Root Cast
Root Cast
6
4
3
2
1
0.0
0.5
1.0
1.5
2.0
2.5
3.0
3.5
4.0
Fault (da
Litholog
• 9S
1300-1425
Charcoal
40
Lithologi

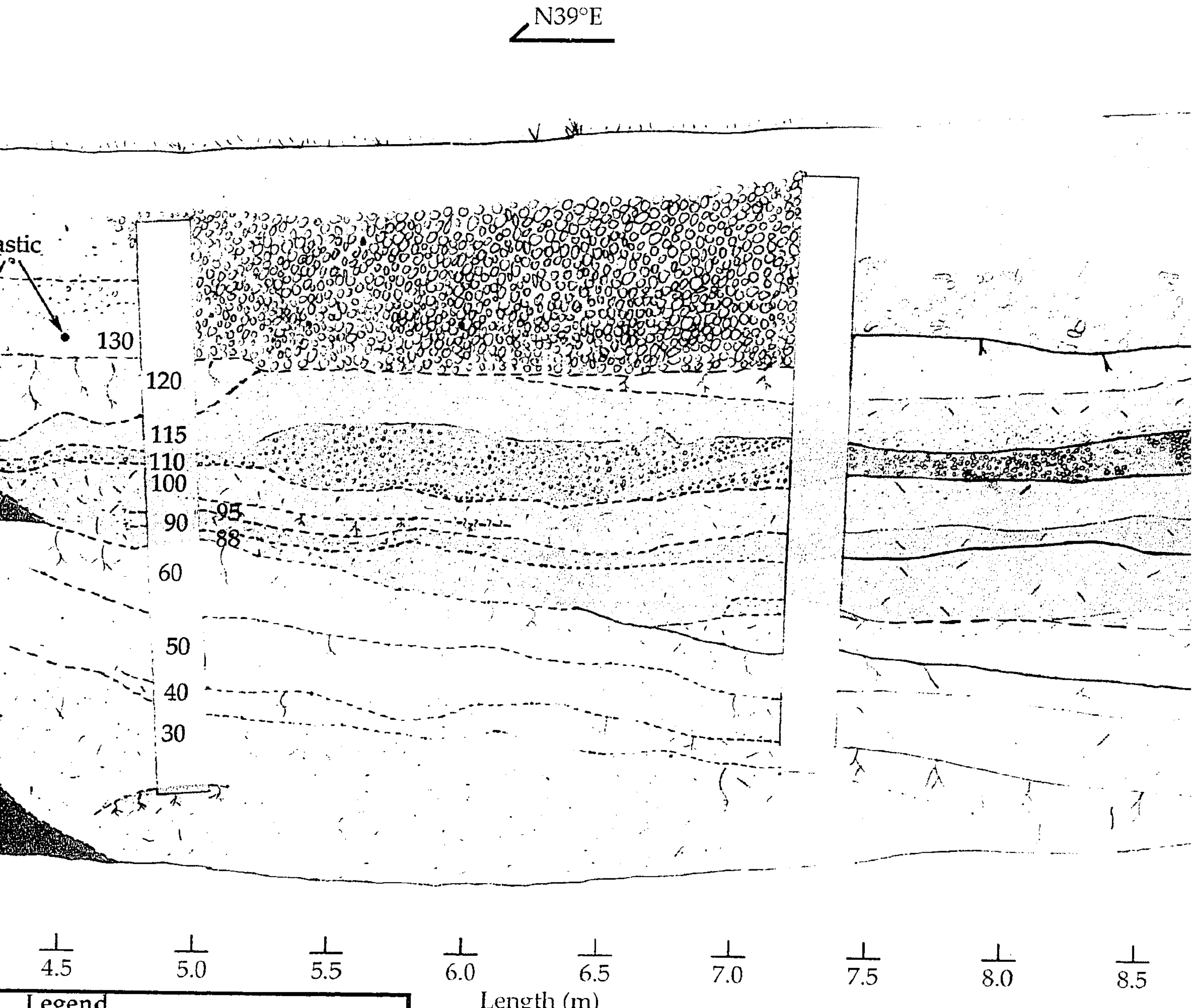

Legend

ed where uncertian)

contact (dashed where uncertain)

ample number and age)

nit number (description on Table 1)

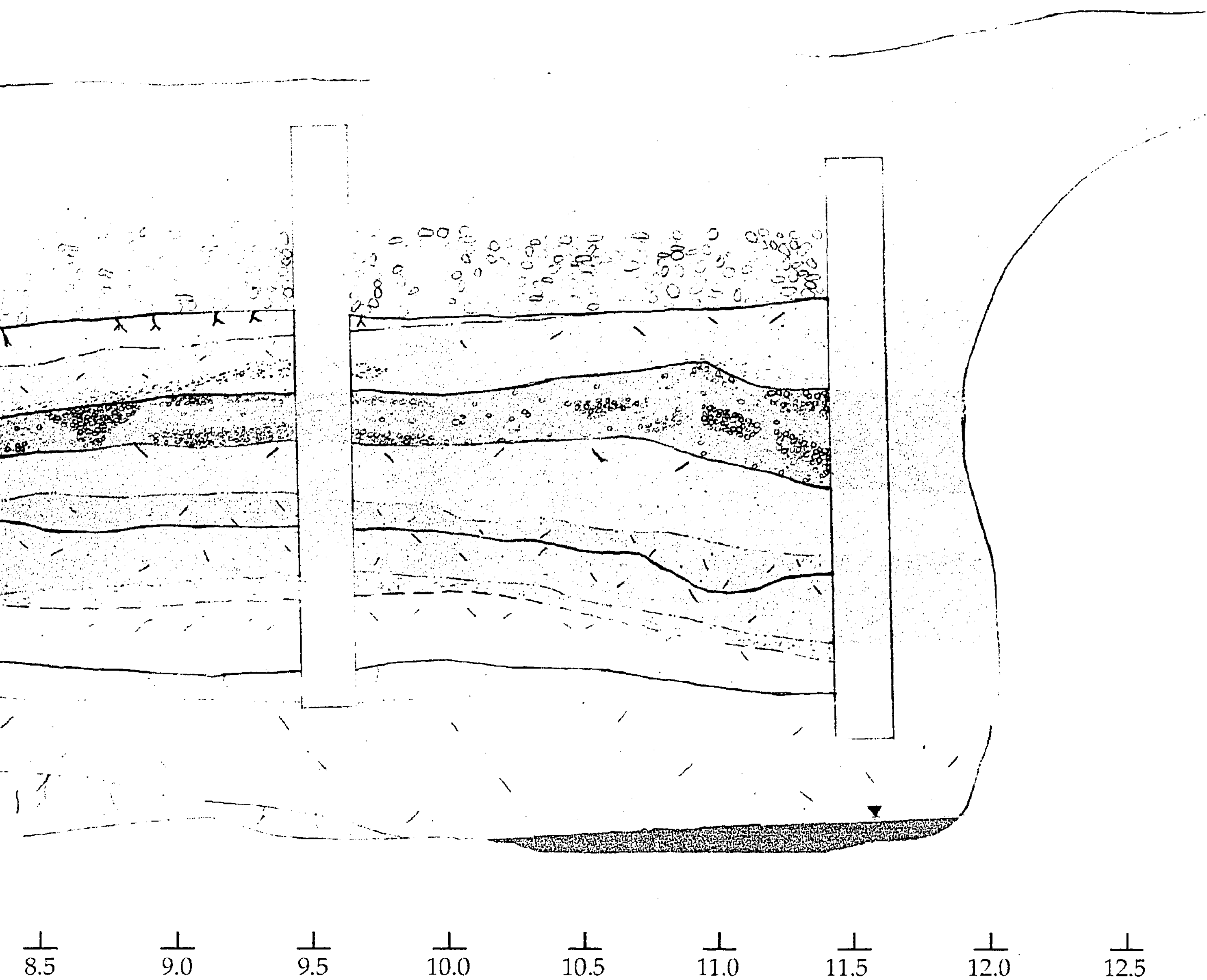

Plate 2. Log of South Wall of Trench T2.

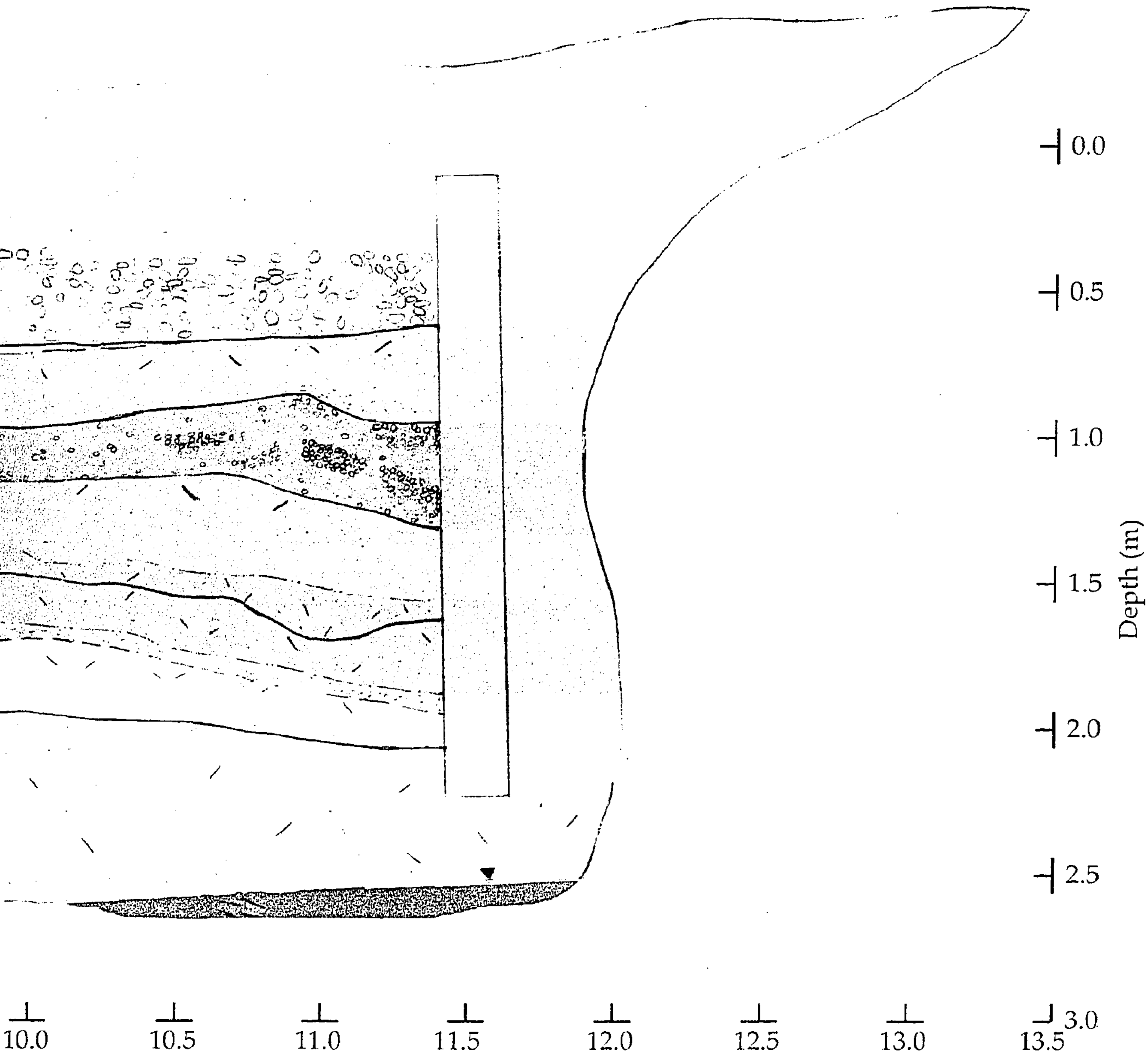

Plate 2. Log of South Wall of Trench T2.